RESULTS

Chapter 3. Results

3.1 Development of probes and establishment of conditions for endocytosis

3.1.1 Preparation of iron-dextran.

Colloidal suspension of iron-dextran using dextran T-40 was prepared in the laboratory using protocol described in section 2.2.1(B). Analysis of the aqueous suspension determined iron content at 10 mg/ml. Stock solution at this concentration was stable for over 2 months at 0°- 4°C, and for more than 7 days at room temperature. Further analysis of the pH stability of the suspension in buffers between pH 2 - 9 showed excellent stability between pH 2 - 8; at higher pH (> pH 8.0), the colloidal iron precipitated with time. The colloidal iron-dextran was stable between temperatures ranging from 4°C to 50°C. The preparation was fully retained by the column matrix (loaded at 0.1 mg/ml for 2 bed volumes) under electromagnetic field and released in its absence (data not shown). Further studies using transmission electron microscopy showed a distinct pattern of dispersed particle clusters of irregular contours. The clusters were made up of individually spaced particles with electron-dense cores approximately 10 nm in diameter surrounded by a thin, diffused electrolucent layer (Fig.1).

3.1.2 Viability of iron-dextran and FITC-dextran fed rat peritoneal macrophages.

Primary cultures of rat peritoneal macrophages incubated with either the commercially available FITC-dextran or the iron-dextran developed in-house – did not show any significant cytotoxic effect at various concentrations tested (except slight cytotoxicity observed in cells exposed to ≥ 3 mg/ml iron-dextran). Various concentrations of each probe resulted in differences in the yield of protein and internalized FITC signals in RF (Table 2). Based on this analysis concentration of

Fig. 1

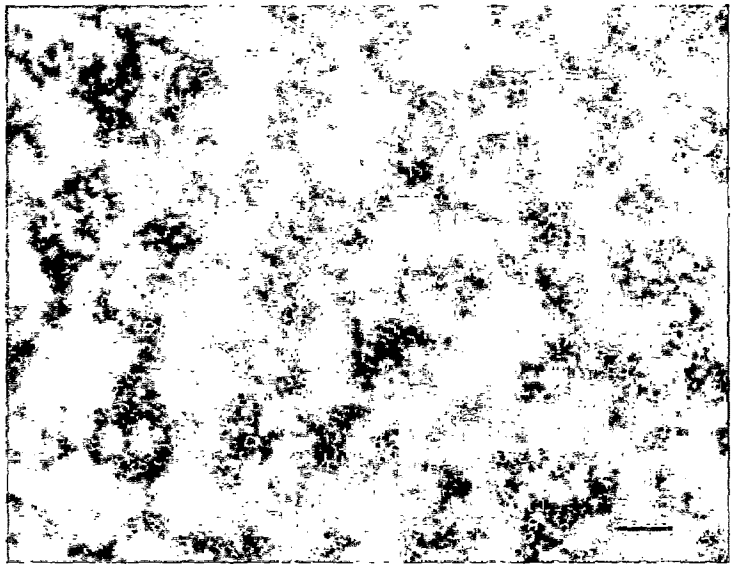

Table 3.

Disruption method	Disruption efficiency *	Acid phosphatase†	
		Supernatant	Intravesicular
Membrane filtration	20	not detected	5.0
Dounce Homogenization	< 95	80	<15
Sonication	< 90	12	70

* Disruption efficiency is expressed as a percentage of cells homogenized by the indicated method.
† values expressed are percentage of total acid phosphatase in the PNS.

Table 2.

Probe	Concentration (mg/ml)	Viable cells (%)	Chromatographic Retention	
			Retained protein*	Retained FITC*
Iron-dextran	1.0	>90	7.0	-
	2.0	>90	20	-
	3.0	80	17	-
FITC-dextran†	0.5	>95	20	49
	1.0	>96	20	65
	2.0	90	20	65
Iron-dextran FITC-dextran	2.0 1.0	>90	20	65

* values expressed are percentage of total PNS constituents retained by the magnetic matrix.
† Iron-dextran was used at a concentration of 2 mg/ml along with FITC-dextran.

1 mg/ml FITC-dextran and 2 mg/ml iron-dextran in DMEM was selected for endocytosis experiments in primary macrophage cultures.

3.1.3 Disruption (homogenization) of rat peritoneal macrophages

Three different disruption techniques were evaluated for optimal subcellular fractionation of rat peritoneal macrophages in order to obtain intact endosome/lysosome preparations (Table 3). The cells when forcibly passed through a series of 5 and 8 μm polycarbonate membrane filters, quickly resulted in clogging of the membranes and incomplete disruption of cells. Analysis of acid phosphatase (marker enzyme for lysosomes) showed only 5% of the total activity in the intravesicular fraction (organelles pelleted following centrifugation) indicating disruption of organelles and release of their contents. Brief homogenization using dounce homogenizer resulted in efficient lysis of macrophages; only 5% of the cells remained intact after homogenization. However, the process also resulted in considerable increase of acid phosphatase activity in the supernatant indicating leakage/damage of subcellular (lysosome/endosome) vesicles. Gentler homogenization decreased the levels of acid phosphatase in supernatant but the efficiency of lysis was much lower (data not shown).

Brief sonication at 4°C for 2 - 3 min at minimum pulse setting resulted in more than 90% lysis of the cells, low release of acid phosphatase in the supernatant and relatively high levels of vesicular (post centrifuge pellet fraction) acid phosphatase, indicating integrity of the vesicles. Subsequent optimization established reproducible protocol [described in section 2.2.3(A.iii)] for efficient harvesting of intact macrophage endosomal vesicles.

3.1.4 Fluid-phase endocytosis of endosomal probes

A. Assay of pinocytic uptake with time

Primary cultures of rat peritoneal macrophages were used to study pinocytic uptake with time, as described in section 2.2.2(A). Briefly, predetermined number of cells ($2x10^6$/well) were incubated in DMEM containing 1 mg/ml FITC-dextran and

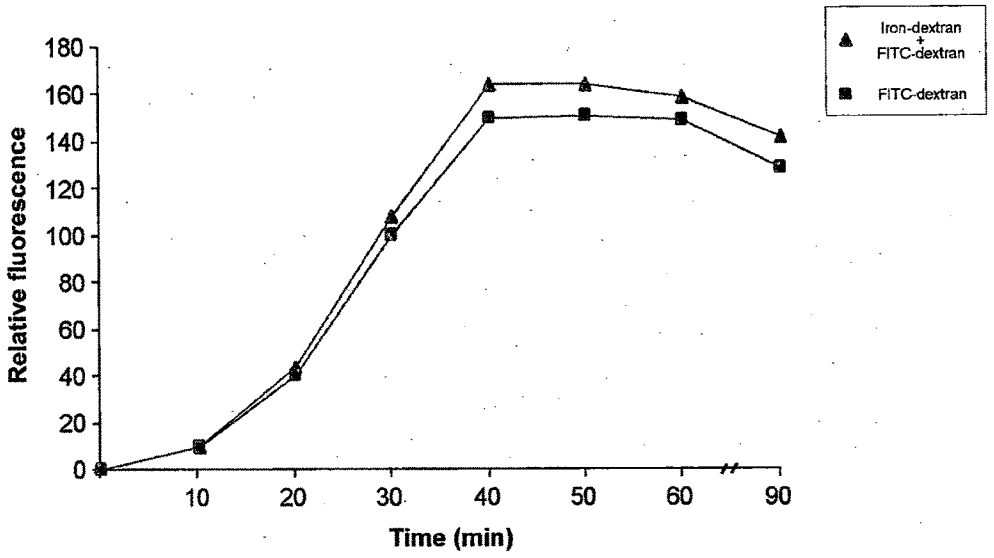

Fig. 2 a.

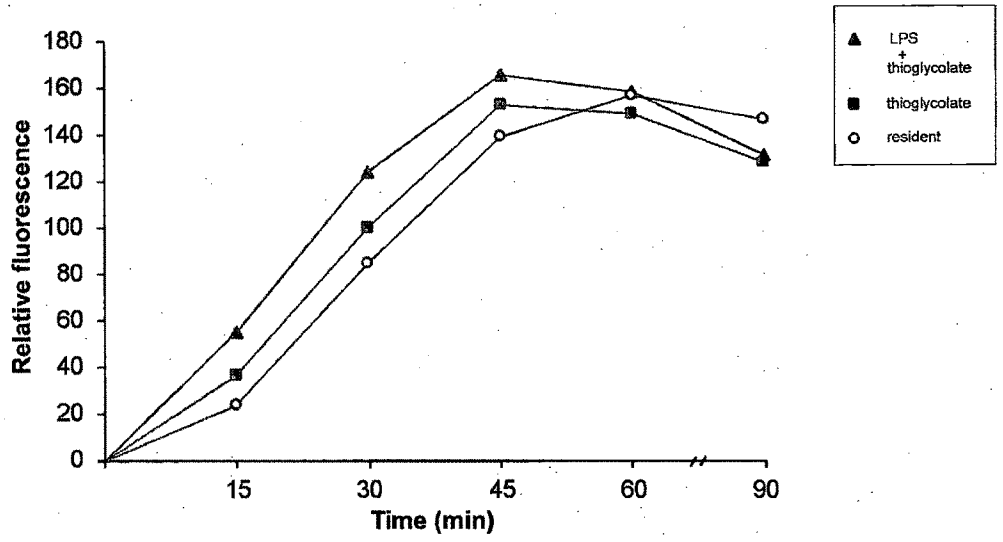

Fig. 2 b.

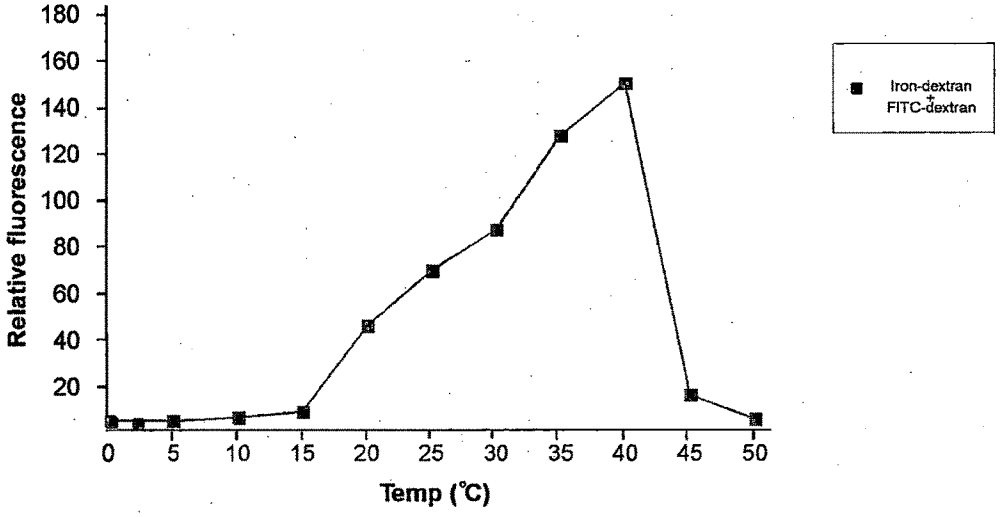

Fig. 2 c.

2 mg/ml iron-dextran for specific (pulse) periods. Plotting the total internalized fluorescence (as a measure of kinetics of FITC-dextran uptake) against pulse time revealed a linear increase of internalized fluorescence up to 45 min, after which there was no further increase (Fig.2b). Resident and LPS induced peritoneal macrophages showed similar uptake kinetics as thioglycolate elicited cells (Fig.2b). Comparison between thioglycolate elicitated cells exposed only to FITC-dextran and to both FITC-dextran and iron-dextran showed comparable uptake of both ligands either individually or together up to 60 min (Fig.2a). Cell viability determined by trypan blue exclusion assay showed > 90% viable cells in all sets (data not shown).

B. Effect of temperature on pinocytic uptake

To determine effect of temperature on endocytic uptake, experiments were conducted as described in section 2.2.2(B). Analysis of internalized fluorescence in cells incubated for 45 min with FITC-dextran and iron-dextran at various temperatures showed that the uptake was essentially absent at 10°C or below and increased concomitantly reaching a peak at 40°C (Fig.2c). There were two inflection points: one at temperatures exceeding 15°C, and the other above 30°C. Further increase in incubation temperature beyond 40°C led to a sharp decrease in pinocytosis. Ultimately no pinocytosis was observed above 45°C (Fig.2c). Cell viability decreased with increase in temperature beyond 45°C (data not shown).

3.2. Purification and characterization of endosomes

3.2.1 Electromagnetic affinity chromatography

The experiments described above helped define optimal conditions for uptake of FITC-dextran and colloidal iron-dextran in primary cultures of rat peritoneal macrophages by fluid-phase pinocytosis. A flow rate of 1 ml/min was optimized for loading and washing the column. The material retained in the column (Retained Fraction or 'RF') typically occupied no more than the top quarter of the steel wire bed. The strong magnetic field (0.8 Tesla) offered excellent retention of the material while the washing (10 bed volumes) step resulted in efficient removal of

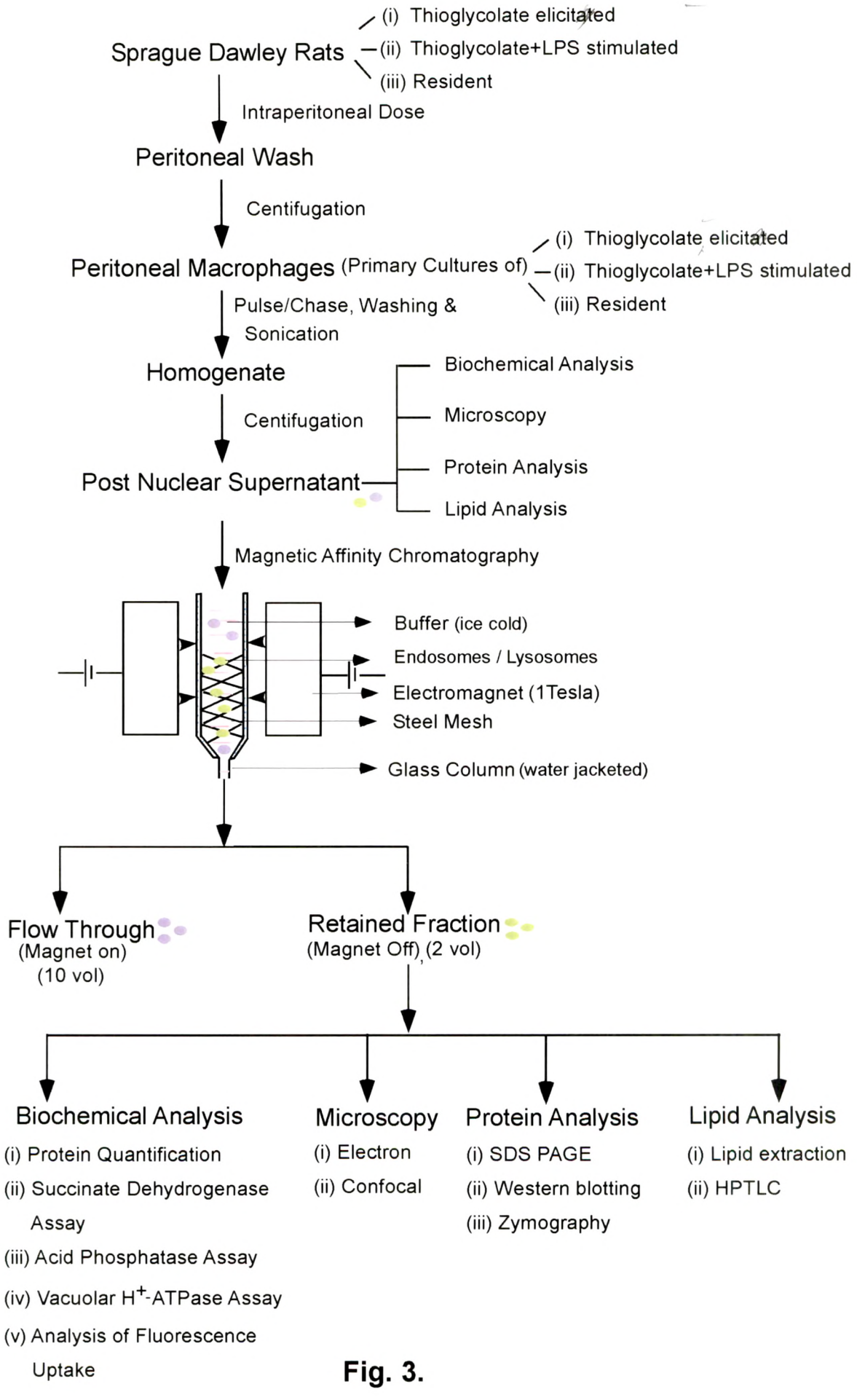
Sprague Dawley Rats
(i) Thioglycolate elicitated
(ii) Thioglycolate+LPS stimulated
(iii) Resident
Intraperitoneal Dose
Peritoneal Wash
Centifugation
Peritoneal Macrophages (Primary Cultures of)
(i) Thioglycolate elicitated
(ii) Thioglycolate+LPS stimulated
(iii) Resident
Pulse/Chase, Washing & Sonication
Homogenate
Centifugation
Post Nuclear Supernatant
Biochemical Analysis
Microscopy
Protein Analysis
Lipid Analysis
Magnetic Affinity Chromatography
Buffer (ice cold)
Endosomes / Lysosomes
Electromagnet (1Tesla)
Steel Mesh
Glass Column (water jacketed)
Flow Through
(Magnet on)
(10 vol)
Retained Fraction
(Magnet Off), (2 vol)
Biochemical Analysis
(i) Protein Quantification
(ii) Succinate Dehydrogenase Assay
(iii) Acid Phosphatase Assay
(iv) Vacuolar H+-ATPase Assay
(v) Analysis of Fluorescence Uptake
Microscopy
(i) Electron
(ii) Confocal
Protein Analysis
(i) SDS PAGE
(ii) Western blotting
(iii) Zymography
Lipid Analysis
(i) Lipid extraction
(ii) HPTLC

Fig. 3.

debris/unbound material. Free iron-dextran bound loosely to the column was removed easily during washing. Finally, a single elution cycle effectively removed more than 90% RF protein after withdrawal of the magnetic field. A flow chart of the electromagnetic column chromatography is given in (Fig.3). Protein and fluorescence analysis determined that the predominant protein of the fraction was intravesicular (pelleted following centrifugation of the RF) indicating the elution process did not damage endocytic vesicles. Fluorescence microscopic analysis showed enrichment of intact fluorescent vesicles in RF [Fig.5 (a,b)].

3.2.2 Dot blot analysis for Rab 5 in RF

Analysis of dot blotted proteins from macrophage whole cell lysate, the corresponding PNS fraction and RF showed prominent dot blot immunoreactivity for endosome marker Rab 5 in the RF, when 10 μg protein was loaded. Rab 5 signal was significantly lower in the PNS fraction and no detectable signal was observed in the lysates when equal amount of protein was loaded (Fig.4b). At lower protein concentrations (5 μg and 3 μg respectively) no detectable signal was observed in either PNS or whole cell lysate, while RF sample showed comparatively lower but noticeable signal. Digital image analysis revealed an average 2 - 3 fold enrichment of Rab 5 in RF after affinity purification compared to respective PNS fraction.

3.2.3 Biochemical analysis of magnetically purified fraction (RF)

Biochemical analysis of endosome-rich RF determined the relative uptake capacity and enrichment of biochemical markers in purified endosomal samples (fraction retained in the magnetic affinity matrix) compared to PNS fraction. The first set of analysis was carried out on cells pulsed for 60 min without chase. The protein content of the RF was approximately one-fifth (19%) of the total PNS protein (Table 4a). Analysis of the lysosomal marker showed 28% of the vesicular acid phosphatase present in the PNS was co-purified during chromatography (Table 4b).

Analysis of purification efficiency of the affinity chromatography technique showed 63% of the total PNS fluorescence was retained and subsequently eluted on

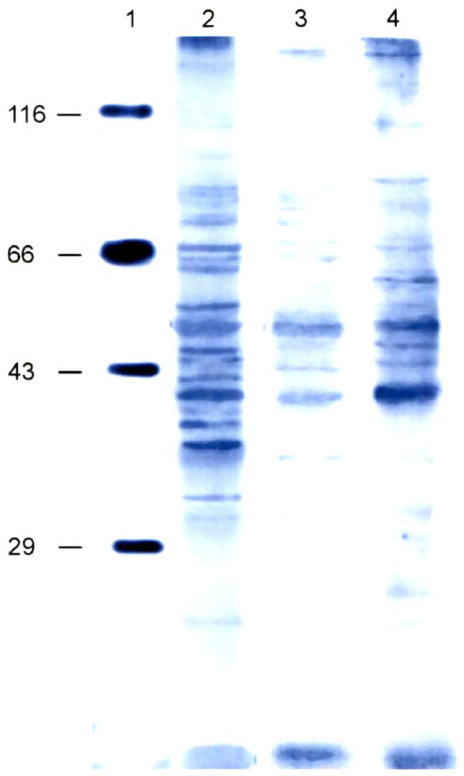

Fig. 4 a.

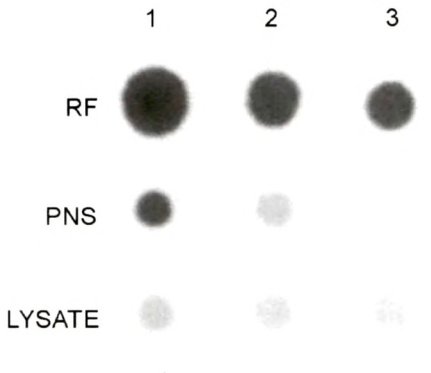

Fig. 4 b.

Table 4 a.

Pulse/Chase	Total cell number	Subcellular fraction	Protein		Lipid	
			Total (µg)	RF*	Total (µg)	RF*
60'/0'	$3x10^7$	**PNS**	3164	18.78	24	8.33
		RF	594		2	

*values expressed are percentage of total PNS constituent present in the purified fraction (RF) following chromatography.

Table 4 b.

Vacuolar H^+-ATPase*	Acid phosphatase*	Succinate dehydrogenase*	rRNA*
55	28	4.26	*n.d.*

*values expressed are percentage of total PNS constituent present in the purified fraction (RF) following chromatography.
n.d = not detected.

Fraction	Total Internalised FITC – dextran	Internalised FITC - dextran *	Specific uptake (Internalized fluorescence / µg protein)	Fold Enrichment
PNS	6588	-	2.08	-
RF	4680	63	7.87	3.78

*values expressed are percentage of total FITC in PNS present in the purified fraction (RF).

Table 4 c.

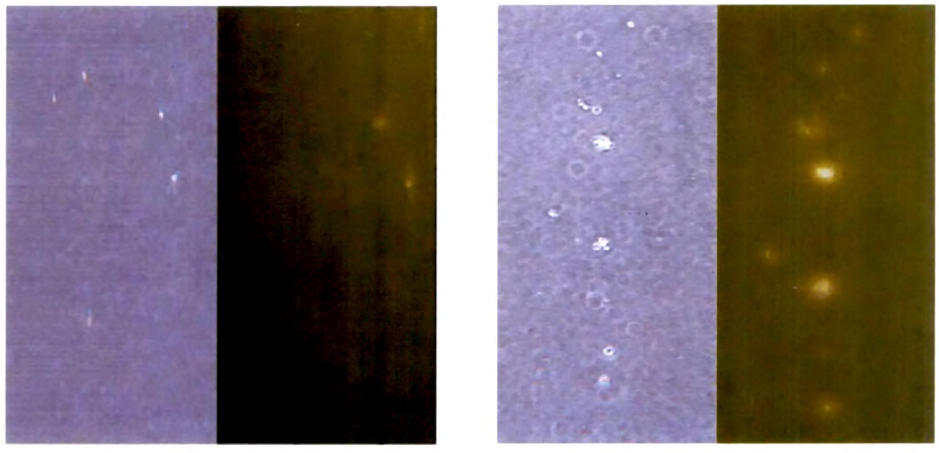

Fig. 5.

affinity magnetic matrix. The RF showed 3.4 - fold enrichment of FITC fluorescence against PNS (Table 4c). The RF did not contain ribosomal RNA indicating absence of contaminating endoplasmic reticulum (ER) (Table 4b). Furthermore, RF contained less than 5% succinate dehydrogenase (mitochondrial marker enzyme) present in the PNS, implying minimal contamination from mitochondria. Conversely, RF samples contained 55% of the vacuolar H^+-ATPase (endosome marker enzyme responsible for acidification) present in the PNS, indicating significant enrichment of endocytic vesicles during purification (Table 4b). In independent experiments, addition of ATP during purification procedure resulted in macroscopically visible clarification of the endosomal preparation (data not shown).

The biochemical characteristics of endosome rich fractions changed with different pulse-and-chase periods (Table 5). In cells pulsed for 5 min without chase, 8% of the PNS protein was retained on the magnetic field; only 6% of the vesicular acid phosphatase was present in the RF. Parallel cells pulsed for 15 min without chase retained 10% PNS protein; with higher levels of vesicular acid phosphatase (12% of that present in the PNS). Independent set of cells pulsed for 5 and 15 min followed by a 30 min chase, showed 24% and 16% of total PNS protein in RF; acid phosphatase in RF increased to 34% of total PNS activity. Further increase in chase periods (60 min chase following 15 min pulse) did not increase the content of RF protein (17%) or levels of intravesicular acid phosphatase (25%). Analysis of purification efficiency of endosomal vesicles with different pulse and chase experiments showed 35% - 80% of the ingested FITC-dextran in the PNS was magnetically retained/purified following electro-magnetic chromatography. Overall the intravesicular FITC-dextran in the RF was enriched by 3 - 5 fold (Table 5).

In resident peritoneal macrophages pulse fed for 5 min without chase, RF contained 7.5% of total PNS proteins and 5.2% of total PNS acid phosphatase. Assays for pinocytic efficiency showed 40% of the FITC-dextran was present in the RF (Table 6).

The biochemical characteristics of LPS stimulated macrophages were also investigated. In cells with 15'/0', 15'/30' and 60'/0' pulse/chase regimens 20%, 26% and 27% of the PNS protein was present in the respective RF's. There was relatively

Pulse/Chase	Total Cell number	Subcellular fraction	Protein*	Internalized FITC-dextran*	Fold enrichment (FITC-dextran)	Acid Phosphatase*	Fold enrichment (Acid Phosphatase)
5'/0'	$3x10^7$	RF	8.4	43	5	6.3	0.76
15'/0'	$3x10^7$	RF	10.2	35	3-4	12.6	1.24
5'/30'	$3x10^7$	RF	24.0	80	3-4	34.5	1.44
15'/30'	$3x10^7$	RF	16.0	48	3	33.0	2.06
15'/60'	$3x10^7$	RF	17.0	52	3	25.0	1.47
60'/0'	$3x10^7$	RF	18.7	63	3-4	28.0	1.49

*values expressed are percentage of total PNS constituent present in the purified fraction (RF) following chromatography.

Table 5.

Pulse/Chase	Total Cell number	Subcellular fraction	Protein*	Internalized FITC-dextran*	Fold enrichment (FITC-dextran)	Acid Phosphatase*	Fold enrichment (Acid Phosphatase)
5'/0'	$3x10^7$	RF	7.50	40	5.33	5.23	0.70

*values expressed are percentage of total PNS constituent present in the purified fraction (RF) following chromatography.

Table 6.

Pulse/Chase	Total Cell number	Subcellular fraction	Protein*	Internalized FITC-dextran*	Fold enrichment (FITC-dextran)	Acid Phosphatase*	Fold enrichment (Acid Phosphatase)
15'/0'	$3x10^7$	RF	20.75	64	3	19	0.92
15'/30'	$3x10^7$	RF	26.00	77	3	20	0.77
60'/0'	$3x10^7$	RF	27.00	79	3	25	0.93

*values expressed are percentage of total PNS constituent present in the purified fraction (RF) following chromatography.

Table 7.

low level of enrichment of acid phosphatase (< 1) in all three sets (compared to the corresponding control sets). Though fluorescent analysis showed, the pinocytic marker FITC-dextran was enriched approximately 3 fold in both LPS stimulated cells and non-LPS controls, the relative purification yield of the fluorescent tagged vesicles was higher with LPS; 64%, 77% and 79% respectively (Table 7).

3.2.4 Determination of intravesicular pH in native and ATP treated endosomes

The intravesicular pH of purified endocytic vesicles was determined as described in section 2.3.3. Correlating the relative fluorescence ratio with the standard curve (Fig.6a), pH of two sets of PNS and endocytic vesicles were analyzed. The intravesicular pH of PNS and purified endosomes from cells pulsed for 15 min with no chase were 6.6 and 6.0 respectively while pH in endosomes and PNS at later stages of the endocytic pathway pulsed for 15 min and chased for 60 min were 4.5 and 5.8, respectively. This was the average pH of the vesicle population since some leaking vesicles may have increased the average pH.

In order to determine the biochemical/functional integrity of the purified endosomes, *in vitro* ATP-dependent vesicular acidification was assessed using endosomes purified from sets pulsed for 15 min and incubated in the presence of ATP as described in section 2.3.4. The initial pH of the system was 6.0 that remained unchanged for 30 seconds. Addition of 1 mM ATP at this point quickly resulted in decrease in FITC fluorescence indicating *in vitro* acidification. The ATP induced acidification was reversed by addition of nigericin at 210 sec. Nigericin resulted in prompt increase of fluorescence (Fig.6b). The fluorescence of FITC-dextran alone was not altered by addition of ATP or nigericin (data not shown). Furthermore, aliquots of the purified endosome fraction pretreated with nigericin (control set) did not show decrease of fluorescence upon addition of ATP while purified endosomes (without ATP) showed increase in fluorescence upon nigericin addition (Fig.6c).

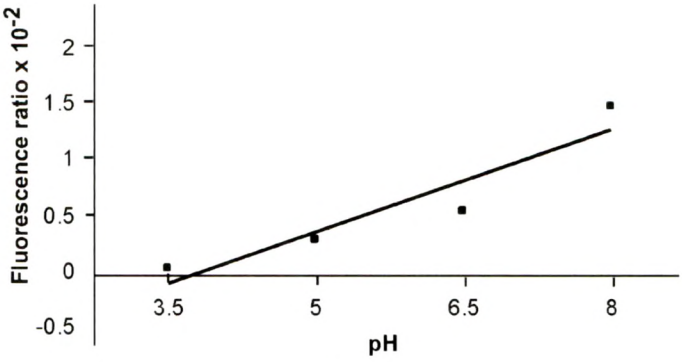

Fig. 6 a.

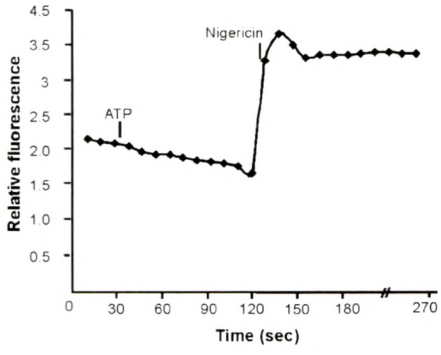

Fig. 6 b.

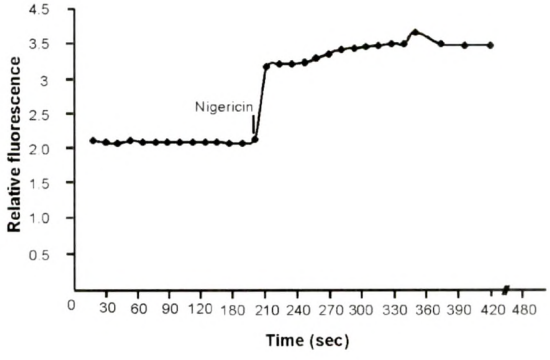

Fig. 6 c.

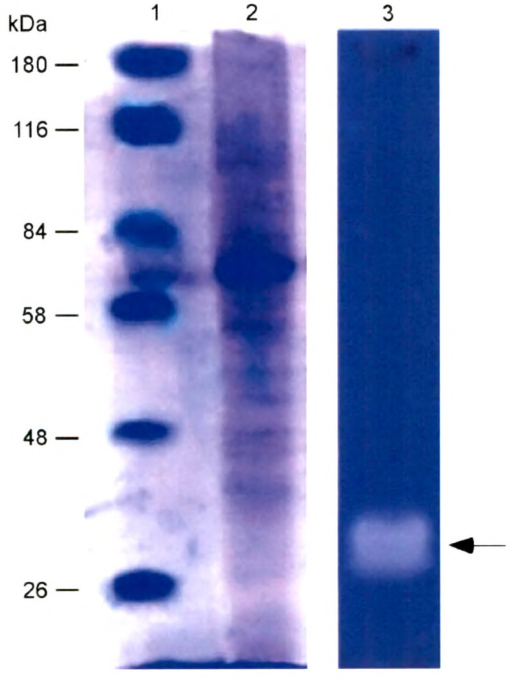

Fig. 7 a.

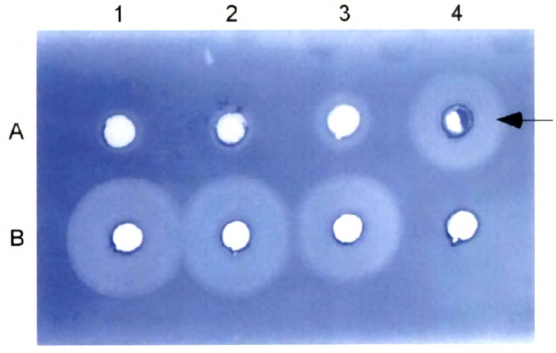

Fig. 7 b.

3.2.5 Electron microscopy

Transmission Electron Microscopy showed a large number of discrete membrane bound vesicular structures in RF (Fig.8). The sample was free from debris and other intracellular organelles (i.e. mitochondria) observed in PNS fractions (data not shown) at low magnification. Negative staining of RF showed comparatively dark electron dense vesicles due to incorporation of iron-dextran. In few cases clusters of iron-dextran particles were clearly discernible inside the lumen (indicated by arrows). Typical organelles from 15'/0' pulsed set were oblong or predominantly cisternal structures between 0.4 μm - 0.8 μm in diameter. Other than the relatively small size as compared to vesicles in the longer pulsed-chased set, many of these structures exhibited an irregular membranous silhouette ranging from spherical, rhomboidal or related structures. The distinguishing feature of this set was a comparative electro-lucent nature of the vesicles compared to the other sets [Fig.8a(i.ii.iii.iv)]. The organelles in longer pulsed-chased set (15'/30') appeared to be more electron dense than the short pulsed sets. Many of these organelles had membranous material inside them [Fig.8b(i.ii.iii.iv.v.vi.vii)]. Few of the vesicles in this set were in the process of fusion and multiple fused vesicles were common [Fig.8b(iii.v.vi.vii)]. The vesicles were between 0.8 μm - 1.6 μm. With an increase in pulse (5'/30', 15'/60') the vesicles became more spherical and electron dense in appearance. All the vesicles in these sets had a dense iron-dextran cluster and were between 0.4 μm - 0.9 μm. Few of the vesicles of these sets were very dark (very late) having characteristic lysosome like appearance [Fig.8(c,d)]. In the last set pulsed for 60 min with no chase the isolated vesicles were 0.5 μm - 1.4 μm in size (Fig.8e).

3.2.6 Protein analysis of RF by SDS - PAGE

The first set of SDS PAGE was used to analyze the protein profiles of cell lysate, the corresponding PNS fraction and RF from resident macrophages pulsed with FITC-dextran and iron-dextran for 60 min. Discrete bands in all three fractions between 10 kDa - 200 kDa were documented for their relative size and intensity. The analysis revealed several bands which were common in all three fractions and unique bands in each fraction that indicated purification of distict proteins in course of magnetic

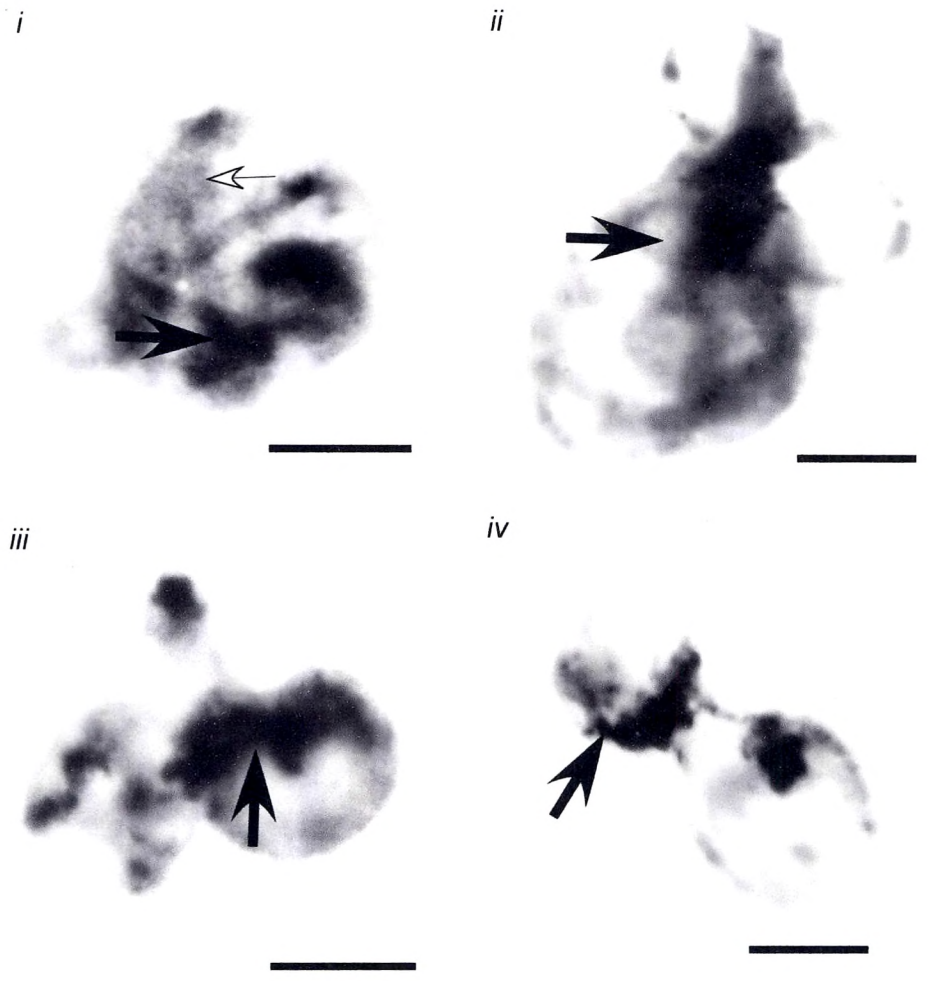

Fig. 8 a.

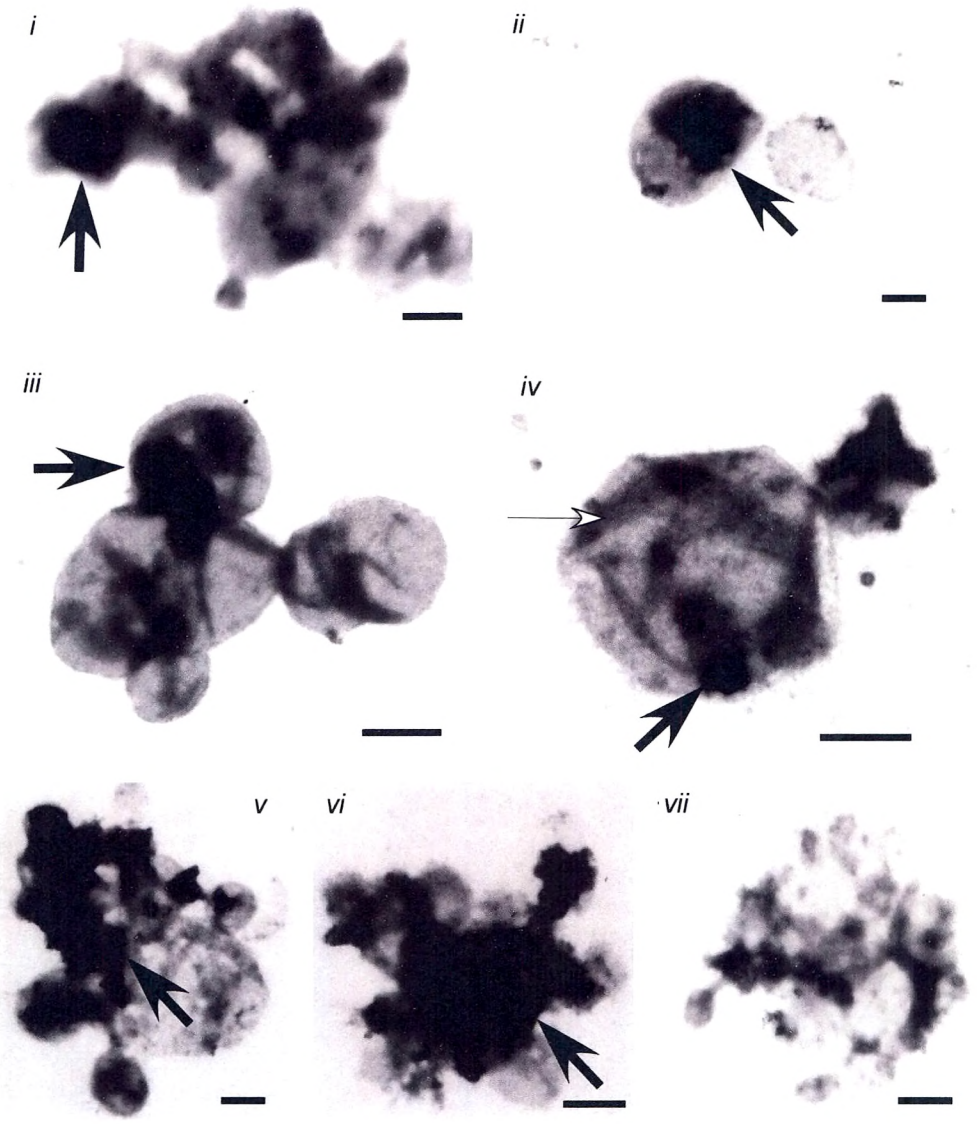

Fig. 8 b.

15/30

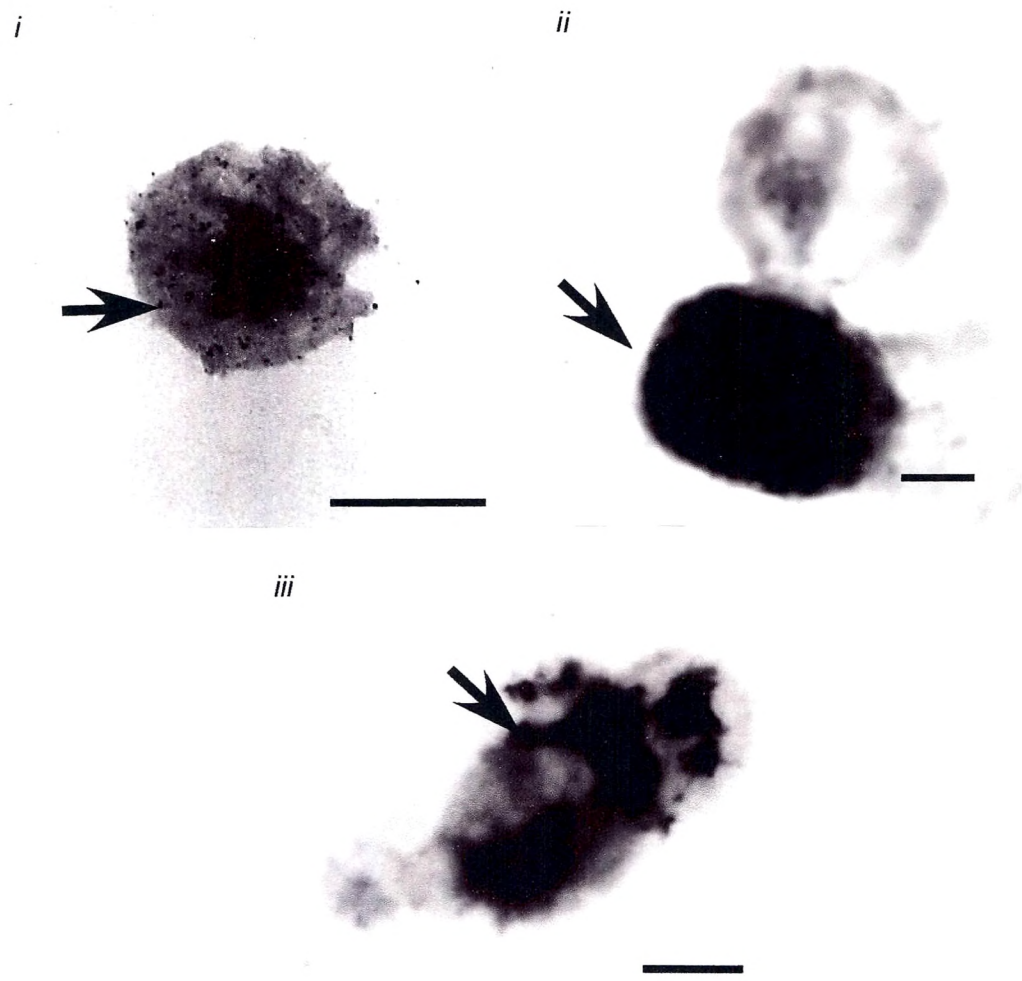

Fig. 8 c.

930

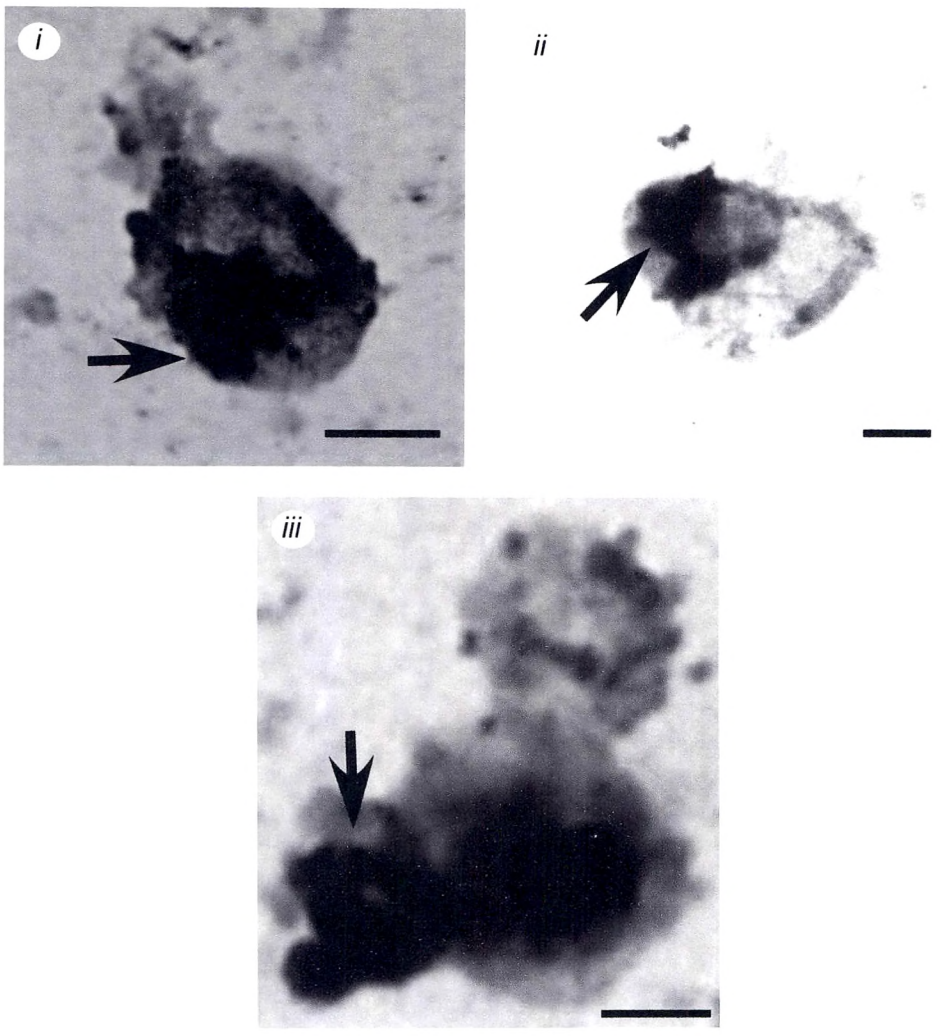

Fig. 8 d.

15760

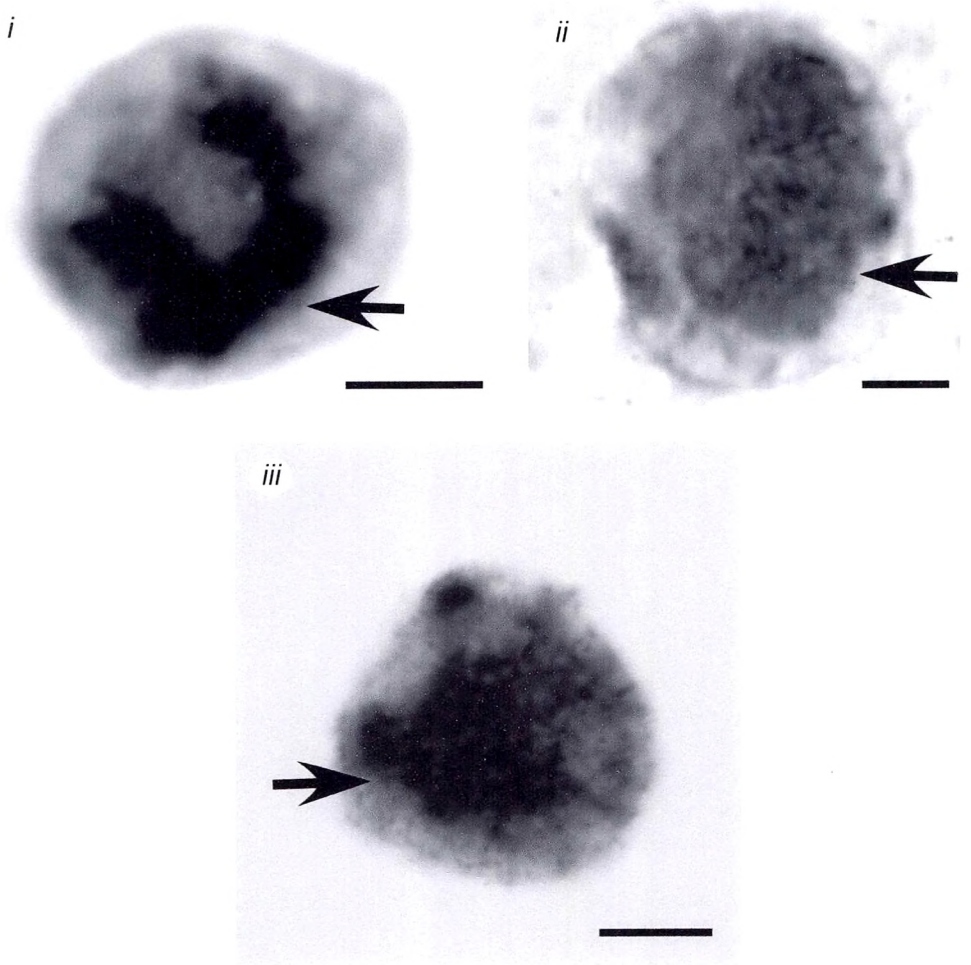

Fig. 8 e.

60/0

chromatography. A new band at ~110 kDa was detected in the RF while several bands at ~70 kDa, ~50 kDa, ~27 kDa, ~26 kDa, ~25 kDa, ~20 kDa, ~18 kDa and ~16 kDa, respectively were present in either the crude lysate or PNS, but were absent in the RF (Fig.4a).

Another set of silver stained PAGE compared protein profiles from corresponding PNS and RF(s) from thioglycolate elicited, resident and LPS stimulated macrophages exposed to identical pulse and chase conditions (Fig.17a). Analysis of the gels for number of bands, their intensities and relative mobilities showed several unique features (Fig.17b).The number of bands in PNS and RF were relatively constant despite the differences in experimental treatments. On an average 30 bands were detected in each set of PNS sample and 27 bands were detected in the RF. Respective bands in RF(s) were assigned numbers according to their relative mobility and color codes were applied to designate proteins/bands in four groups: (a) bands present only in RF (and not in the corresponding PNS), (white), (b) bands common to two sets of RF(s) (blue), (c) bands unique to one set of sample, and (d) bands, which were common to all samples (none). Overall, 25%, 48% and 46% bands in the RF of resident, thioglycolate and LPS stimulated macrophages were unique from their corresponding PNS fractions. Among RF(s) ~81%, ~59% and ~67% of the total protein bands were common among the resident, thioglycolate and LPS group (Table 8). Two clusters of bands, one between 116 kDa - 55 kDa and the other between 46 kDa and 29 kDa showed differences in migration despite overall similarity in their patterns (Fig.17a). Another interesting feature of the analysis was the observation of a ~29 kDa band (#22) in the resident macrophage (in both PNS and RF, with enrichment in RF) that was conspicuously low in other sets (Fig.17a).

3.2.7 Analysis of proteolytic activity in endosome fractions

The total proteolytic activity was analyzed by agar radial diffusion assay using hemoglobin as substrate. Clear zones were observed in wells incubated with affinity purified endosome samples indicating proteolytic activity which was absent when identical samples were treated with broad-spectrum protease inhibitor cocktail, indicating complete inhibition of proteases (Fig.7b). The activity was not inhibited in

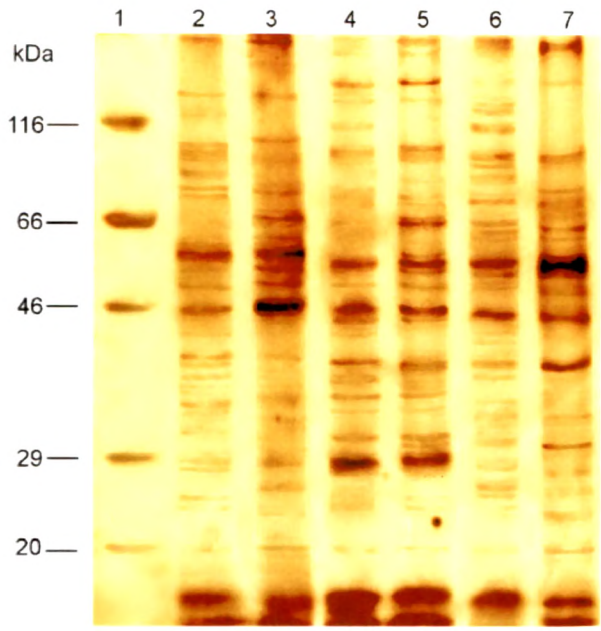

Fig. 17 a.

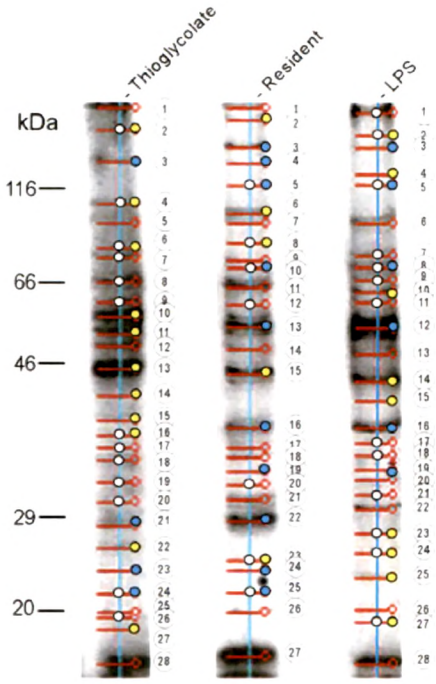

Fig. 17 b.

Type of stimulus	% Similarity*	
	Corresponding PNS	Other Endosome fractions
None (Resident)	74.1	81.5
Thioglycolate	51.9	59.3
LPS	53.6	67.9

*expressed as % of bands in the endosome fraction co-migrating with corresponding PNS or endosome fractions.

Table 8.

samples incubated with PMSF or EDTA. Incubation with leupeptin showed decrease in total proteolytic activity; whereas pepstatin and E-64 significantly inhibited the proteolytic activity. Further analysis of the proteases by zymography (hemoglobin as a substrate) confirmed that significant proteolytic bands were between 25 kDa - 30 kDa (Fig.7a). Proteolytic activity was also detected (comparatively weakly) using gelatin as substrate. Gelatin zymography showed diffused higher molecular weight (~100 kDa) bands (data not shown).

3.2.8 Immuno identification of endosomal proteins by western blot analysis

A. Analysis of major endosome markers and proteases

The first set of Western blot analyzed the PNS fraction(s) and their corresponding RF(s) for the presence of characteristic endosome markers. In order to achieve equilibrium distribution of the iron probe in endosomes of all stages along the endocytic pathway, primary cultures of rat peritoneal macrophages were pulsed with FITC-dextran and iron-dextran for 60 min. Subsequent analysis for Rab 5 revealed a discrete ~23 kDa band in both PNS and RF [Fig.9(i)]. Further analysis by Kodak Image Analysis™ showed 1.5 - fold higher intensity of Rab 5 in RF compared to PNS. Re-probing the blots for Rab 7, revealed a faster migrating ~22 kDa immunoreactive band in both samples, with 3.3 - fold higher signal in RF compared to PNS [Fig.9(ii)]. Analysis of similar blots for the lysosome marker LAMP-1 showed ~120 kDa band with 2 - fold higher signal in PNS than RF [Fig.9(iii)]. Similar analysis was carried out to investigate the nature of major endosome/lysosome related proteases under comparable conditions. Analysis for Cathepsin B, showed a prominent ~30 kDa band in both PNS and RF with a 1.2 - fold higher signal in the latter [Fig.9(v)]. Similar analysis for Cathepsin D showed two prominent bands at ~43 kDa and ~28 kDa in both lanes [Fig.9(vi)]. Both bands were noticeably higher in RF (intensity being 2.3 times and 3.5 times higher, respectively, compared to signals in PNS fraction). Finally reprobing the blots for Cathepsin H

Nice Westerns.

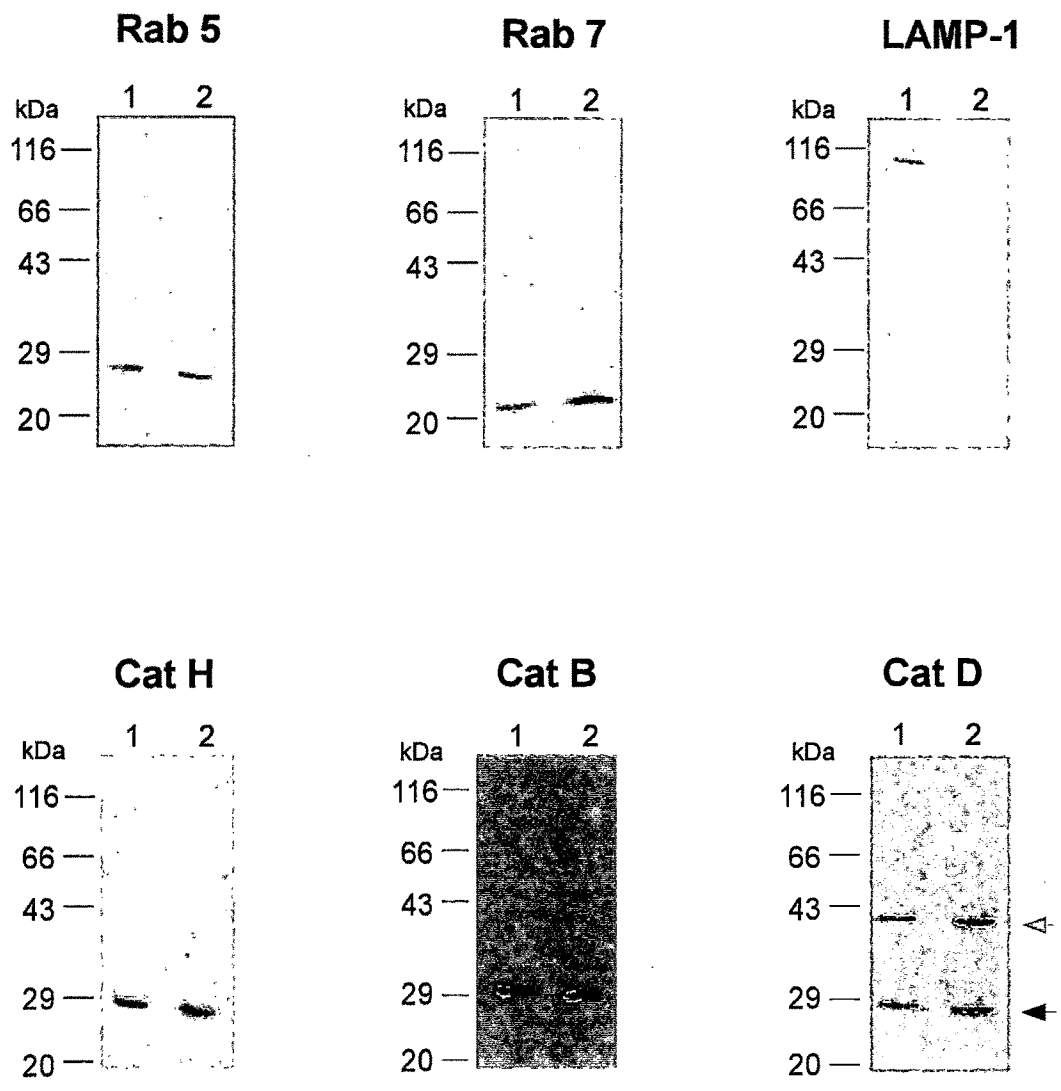

60/0 all

Fig. 9.

showed a single ~27 kDa band with 1.2 - fold higher intensity in RF than the corresponding PNS [Fig.9(iv)].

B. Western blot analysis of the temporal dynamics of endosome markers and major proteases

The next set of Western blot analyzed the expression of endosome markers and proteases in different subsets of endosomes along the endocytic pathway. Four pulse-and-chase conditions were chosen in order to study different classes of endosomes: (i) 5 min pulse without chase (5'/0'), (ii) 15 min pulse without chase (15'/0'), (iii) 15 min pulse with 30 min chase (15'/30'), and (iv) 15 min pulse with 60 min chase (15'/60').

Probing blots for Rab 5 showed the characteristic ~23 kDa band at relatively higher concentration in the short (5' and 15' pulse without chase) pulsed fractions; signal was not detected in the longer pulse-and-chased (15'/30' and 15'/60' respectively) cells (Fig.10a). The Rab 5 signal in corresponding PNS fractions were lower than RF as observed earlier (4.5 - fold lower than corresponding RF in the 15'/0' set). The comparative histogram profile of Rab 5 in RF at the indicated pulse-and–chase condition is shown in Fig.10b(i).

In contrast to Rab 5, the temporal profile of Rab 7 was markedly different. The Rab 7 specific ~22 kDa band was absent in both the fractions of the short pulsed (5'/0') cells. Subsequently, Rab 7 was detected only in the PNS fraction of the (15'/0') set. The signal for Rab 7 was dramatically high in the RF of the 15'/30' set (10 - fold higher in the RF compared to the PNS) and continued to be significantly present in the 15'/60' set (Fig.10a). The comparative histogram profile of Rab 7 in RF at the indicated pulse-and–chase condition is shown in Fig.10b(ii).

The next set of immunoanalysis investigated the expression of LAMP-1. The latter was not detectable in the sets pulsed for shorter periods (5'/0', 15'/0'). LAMP-1 immunoreactive band was observed in the 15'/30' set and more predominantly in the 15'/60' set (data not shown) and 60'/0' set (Fig.10a) indicating association of this marker with the later stages of the endocytic pathway.

The temporal analysis for proteases revealed significant differences between the expression patterns of the cysteine proteases like Cathepsin H and B. The former

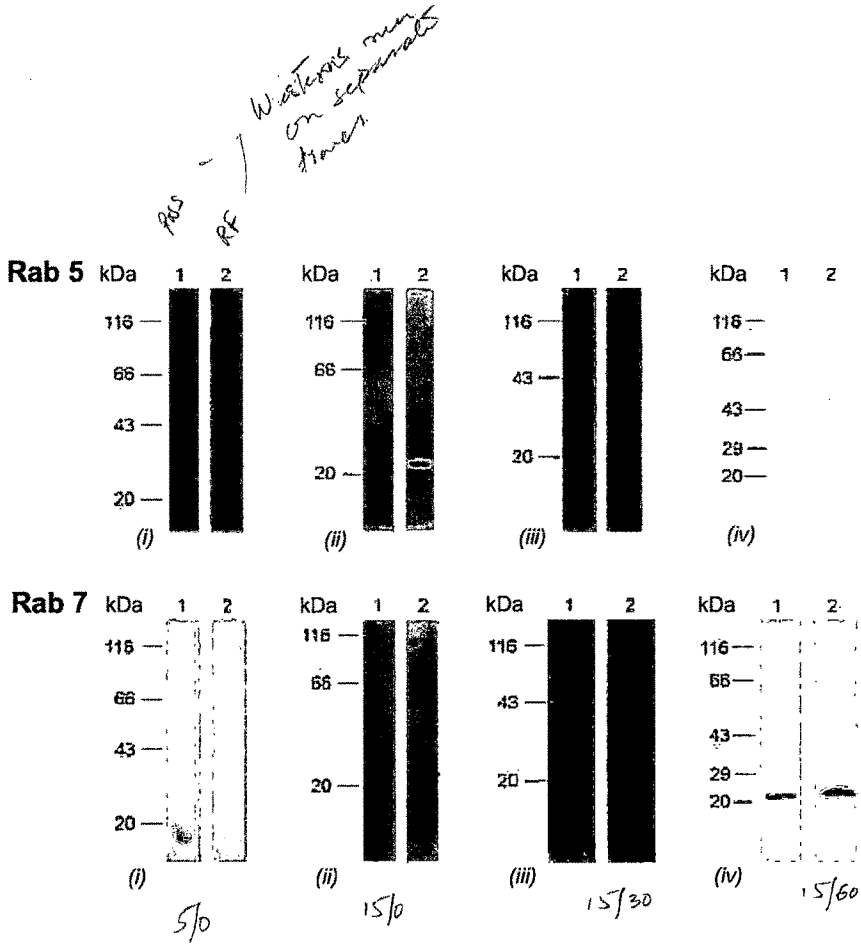

Fig. 10 a.

cont in next page.....

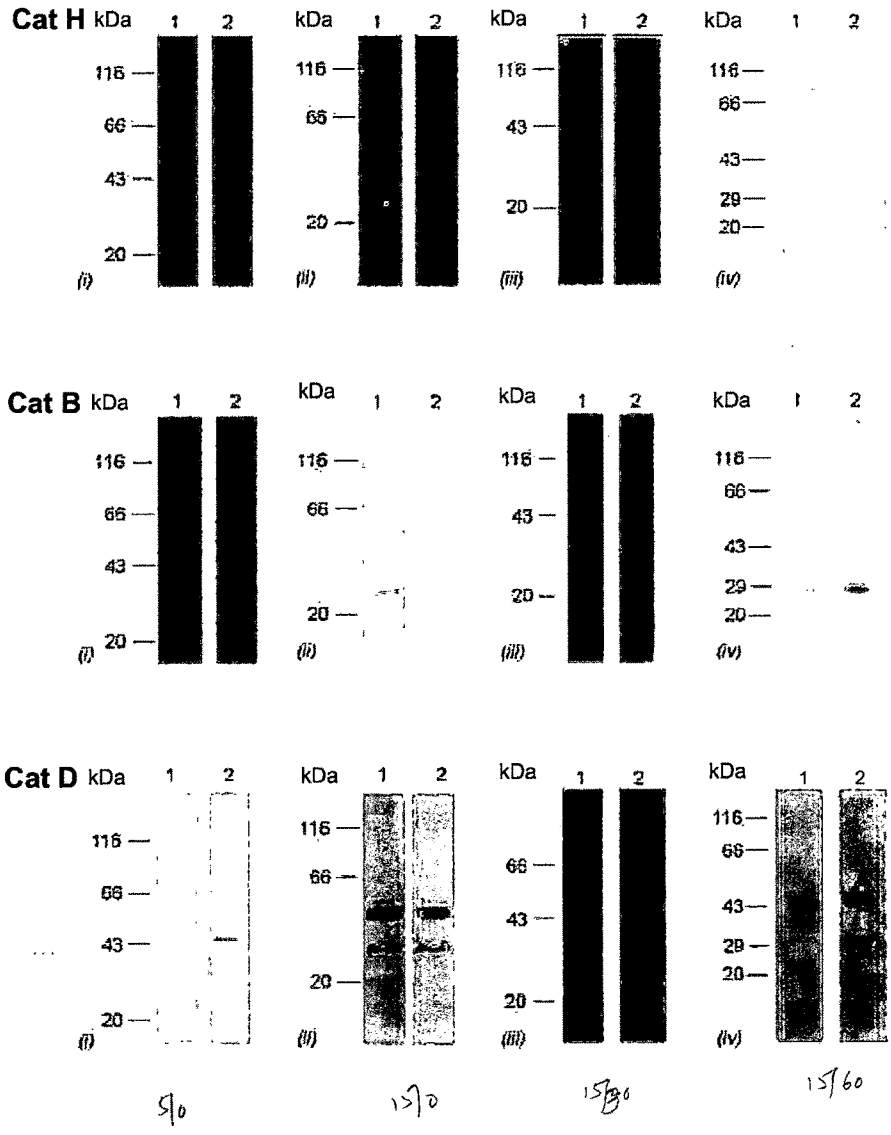

5/0 15/0 15/30 15/60

.....**Fig. 10 a.** **continued.**

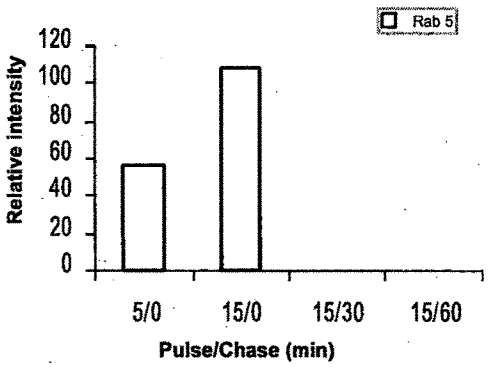

i

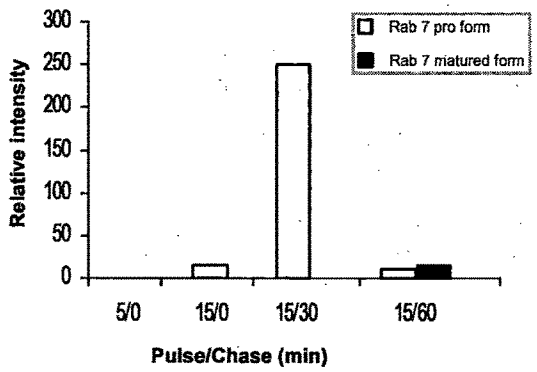

ii

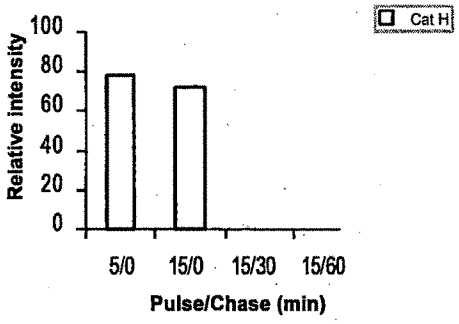

iii

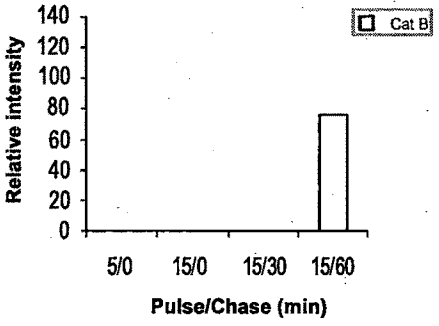

iv

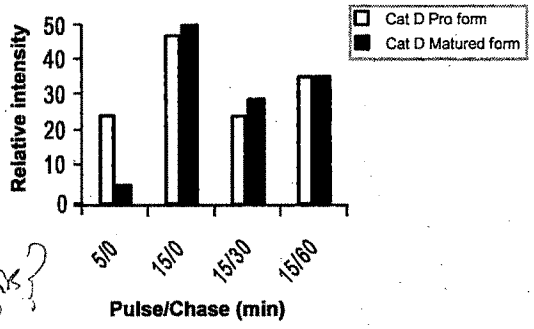

v

Fig. 10 b.

was significantly present in the sets pulsed-and-chased for shorter periods and absent in the sets chased longer, indicating association with early endosomes. Digital quantitation of the bands determined a 10 - fold increase in Cathepsin H signal in RF compared to PNS in 5'/0' pulsed cells. The signal for Cathepsin H remained consistently high in RF of 15'/0' pulsed cells, whereas no signal was observed in the corresponding PNS fraction. In cells exposed to longer chase periods (15'/30' and 15'/60'), Cathepsin H signal was insignificant (Fig.10a). The comparative histogram profile of Cathepsin H enrichment in RF at the indicated pulse-and–chase condition is shown in Fig.10b(iii). Although Cathepsin B was detected in PNS fractions from 5'/0', 15'/0' and 15'/60' pulsed cells, the signal was detected only in RF of the 15'/60' set indicating the selective association of Cathepsin B with late endosomes. The signal for Cathepsin B was ~6 - fold higher in RF than PNS (Fig.10a). The comparative histogram profile of Cathepsin B in RF at the indicated pulse-and–chase condition is shown in Fig.10b(iv).

Whereas the two cysteine proteases showed marked variation in their temporal association, signal for the acid protease Cathepsin D remained relatively constant in all sets. In RF pulsed for 5 min without chase, the ~43 kDa band for Cathepsin D was 2.5 times higher, whereas the mature ~28 kDa band was 1.27 times lower in RF, respectively. Longer pulse periods resulted in concomitant increase in Cathepsin D in both PNS and RF as evident in the 15'/0' set. The comparative profile of both bands of RF and PNS were similar to that observed in the 5'/0' set. In the 15'/30' set both forms of Cathepsin D were present only in RF, whereas in 15'/60' set only a ~43 kDa proform was detected in PNS fraction (Fig.10a). The comparative histogram profile of Cathepsin D in RF at the indicated pulse-and–chase condition is shown in Fig.10b(v).

C. Western blot analysis of endosomal markers in resident macrophages

The next phase of immunoanalysis examined the differences between resident and thioglycolate elicited macrophages (Fig.11). Macrophages from both conditions were pulsed for 5 min and analyzed for expression of major Rab markers and proteases in their endosomal vesicles. The analysis revealed 1.1 - fold higher levels of Rab 5 in

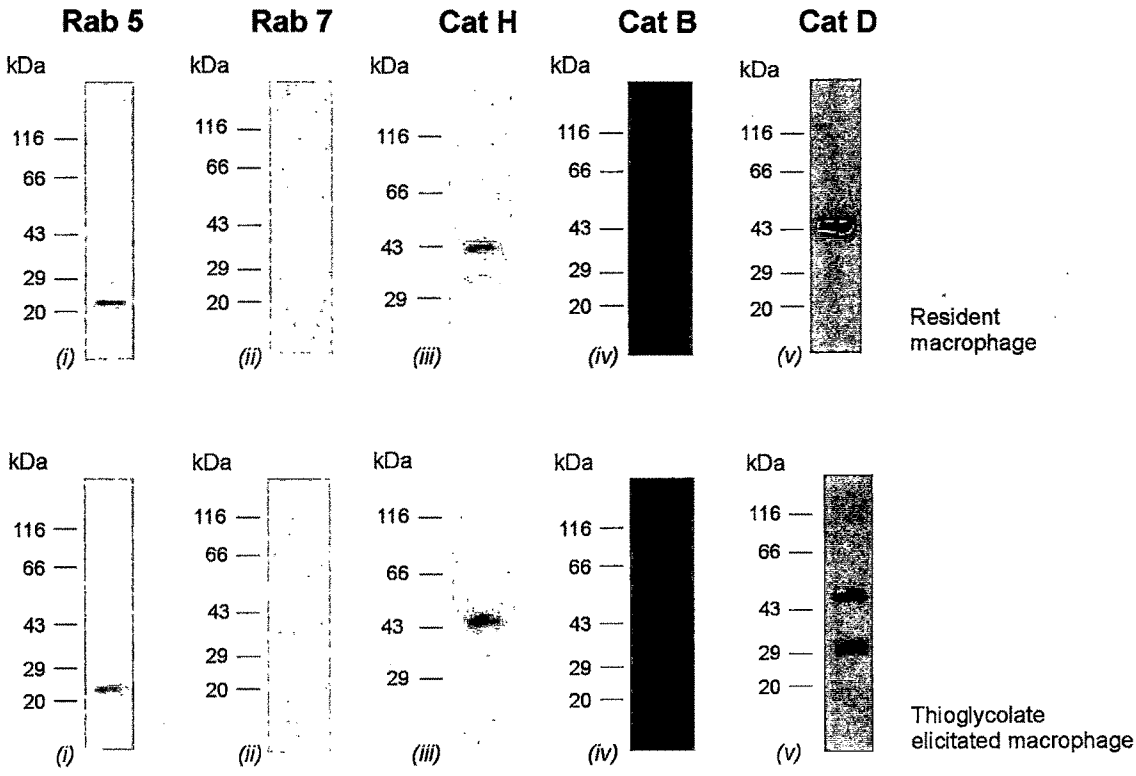

Fig. 11 a.

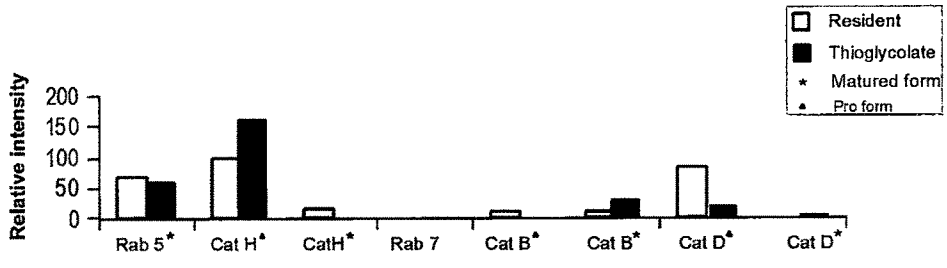

Fig. 11 b.

resident macrophage endosomes relative to the thioglycolate elicited macrophages [Fig.11a(i)] whereas the late endosome marker Rab 7 was not detected in either set [Fig.11a(ii)]. A prominent signal for Cathepsin H proform at ~43 kDa and a less intense faster migrating ~33 kDa form was detected in the resident macrophage endosomes; the proform was also detected in thioglycolate elicited macrophages [Fig.11a(iii)]. Immunoanalysis of Cathepsin B in resident macrophages determined a ~40 kDa proform, apart from the more frequently observed ~30 kDa form. The corresponding thioglycolate elicited set showed higher levels (3.8 - fold higher intensity) of only the mature ~30 kDa form of Cathepsin B [Fig.11a(iv)]. Analysis for Cathepsin D showed a prominent single band at ~43 kDa in resident macrophage endosomes, and two bands in the thioglycolate elicited set [Fig.11a(v)]. The comparative histogram profile (5'/0' set) of the indicated proteins and proteases in RF between resident and thioglycolate elicited macrophages is shown in Fig.11(b).

D. Western blot analysis for endosomal markers in LPS stimulated macrophages

The final set of Western blots analyzed the temporal expression of endosome markers/proteases in RF from primary cultures derived from rats exposed to inflammatory stimuli (LPS) as compared to control rats exposed to only thioglycolate and no LPS.

Comparison between lanes loaded with equal amount of proteins showed Rab 5 to be 3.8 - fold more abundant in control RF(s) than their LPS induced counterparts at 15 min pulse [Fig.12a(i)]. The signal for Rab 5 increased significantly at later time points: there was prominent signal for Rab 5 in 15'/30' sets compared to control sets where no Rab 5 was detected [Fig.12a(ii)] and also in 60'/0' sets where Rab 5 was 2.4 - fold higher than control sets [Fig.12a(iii)]. The comparative histogram profile for Rab 5 in RF, between LPS stimulated and thioglycolate elicited macrophages, at indicated time points is shown in Fig.12(b).

Comparison between the temporal profiles of Rab 7 indicated a relatively slower rate of endosomal maturation in LPS induced macrophages. Whereas no Rab 7 was detected in the 15 min pulsed set even after 30 min chase in LPS sets, significant levels of Rab 7 was detected in (15'/30') control sets [Fig.13a(i,ii)]. The profile of Rab

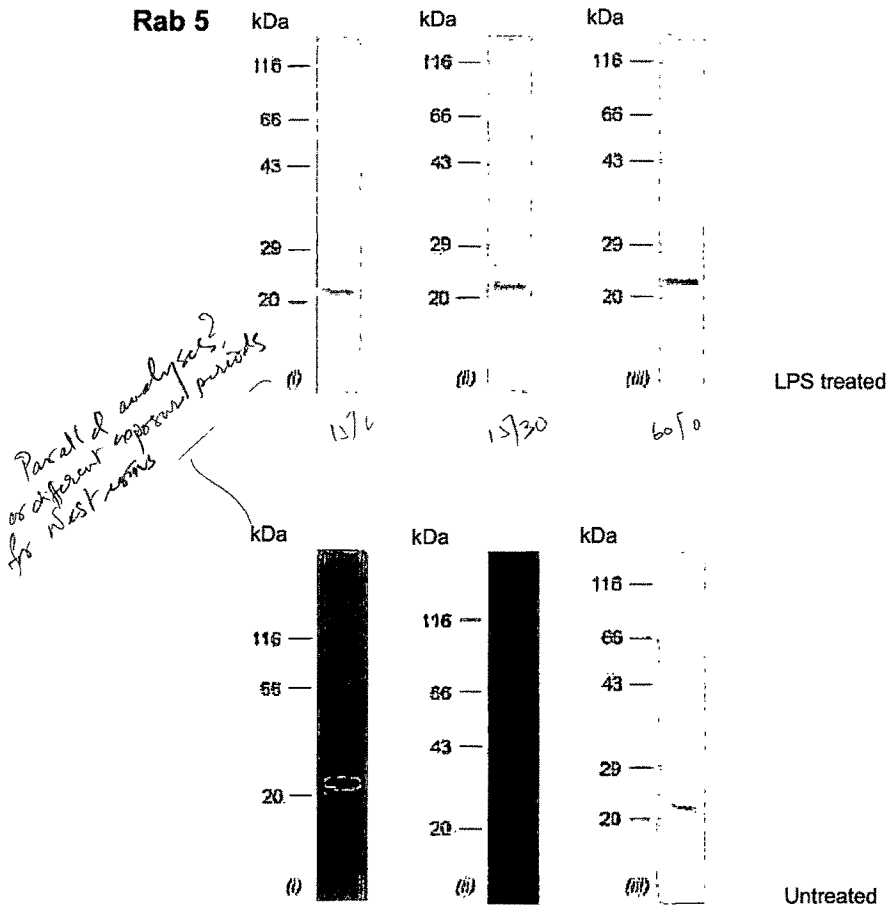

Fig. 12 a.

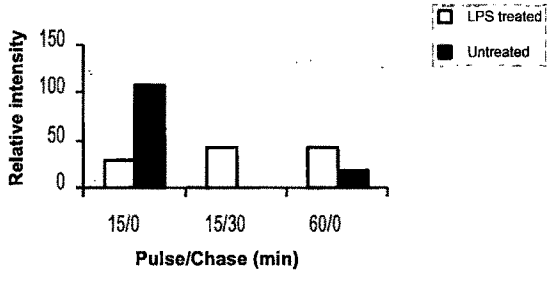

Fig. 12 b.

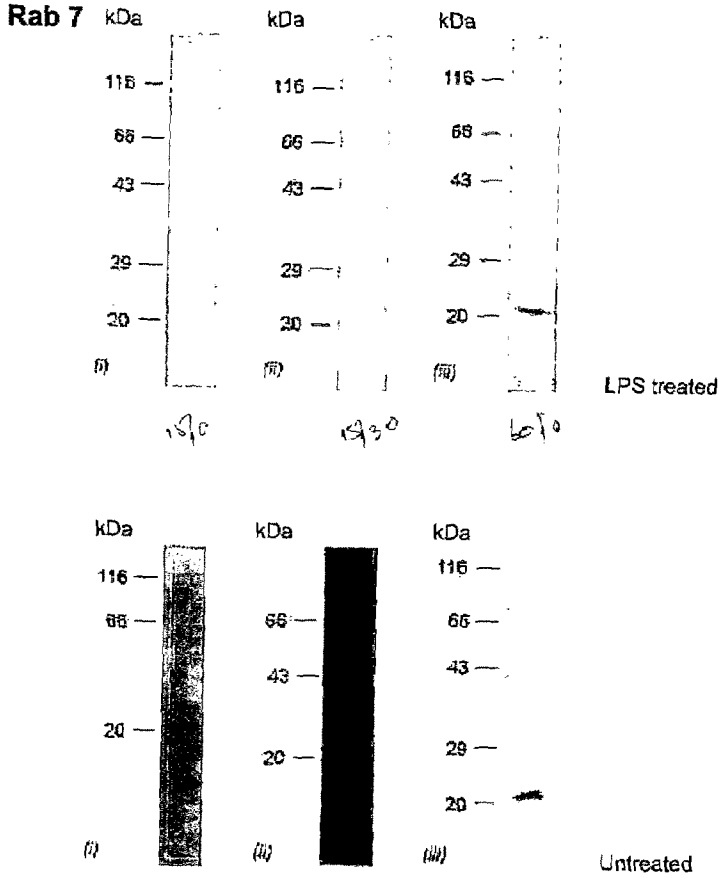

Fig. 13 a.

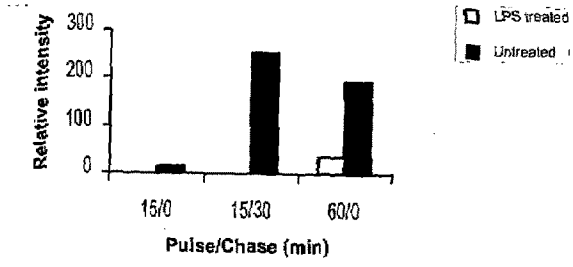

Fig. 13 b.

7 was also evident in 60 min pulse: there was 5 - fold higher expression of Rab 7 after a 60 min pulse in control sets than LPS induced ones [Fig.13a(iii)]. The comparative histogram profile for Rab 7 in RF, between LPS stimulated and thioglycolate elicited macrophages, at indicated time points is shown in Fig.13(b).

Analysis for Cathepsin H profile depicted dramatic differences between thioglycolate elicitated controls and LPS induced cells. In LPS induced macrophages, Cathepsin H was observed even after 30 min chase wherein its activity dropped slightly by 10% relative to its maximal level just after 15 min of pulse. In non-induced controls maximum levels (1.2 fold higher than the corresponding LPS set) of Cathepsin H was detected immediately after 15 min pulse which soon dropped down to undetectable limits after 30 min of chase [Fig.14a(i,ii)]. In consistence with the delayed maturation kinetics, 60'/0' LPS induced macrophages showed 3.2 - folds higher levels of Cathepsin H than corresponding controls [Fig.14a(iii)]. The comparative histogram profile for Cathepsin H in RF, between LPS stimulated and thioglycolate elicited macrophages, at indicated time points is shown in Fig.14(b).

In case of Cathepsin B, signals were detectable in early 15'/0' LPS induced set, which increased by 2 and 2.4 - fold in 15'/30' and 60'/0' sets, respectively [Fig. 15a(i,ii,iii)]. In contrast, in control Cathepsin B signal was only observed in the later 60'/0' pulsed set, however the signal for the latter was 2.4 - fold higher in the control than its LPS induced counterpart [Fig.15a(i,ii,iii)]. Interestingly, the 60'/0' LPS induced set also showed a ~27 kDa proform which was 8.3 - fold higher than its corresponding ~25 kDa mature form [Fig.15a(iii)]. The comparative histogram profile for Cathepsin B in RF, between LPS stimulated and thioglycolate elicited macrophages, at indicated time points is shown in Fig.15(b).

Immunoreactivity for the aspartyl protease Cathepsin D was detected in all control and LPS induced sets at comparable levels (Fig.16a). In LPS induced sets the ~40 kDa proform was slightly higher (1- fold) than corresponding ~27 kDa mature form in the 15'/0' sets [Fig.16a(i)]. After 30 min chase, level of the mature form increased 1.3 times than the proform [Fig.16a(ii)]. The comparative histogram profile for Cathepsin D, in the RF, between LPS stimulated and thioglycolate elicited macrophages, at indicated time points is shown in Fig.16(b).

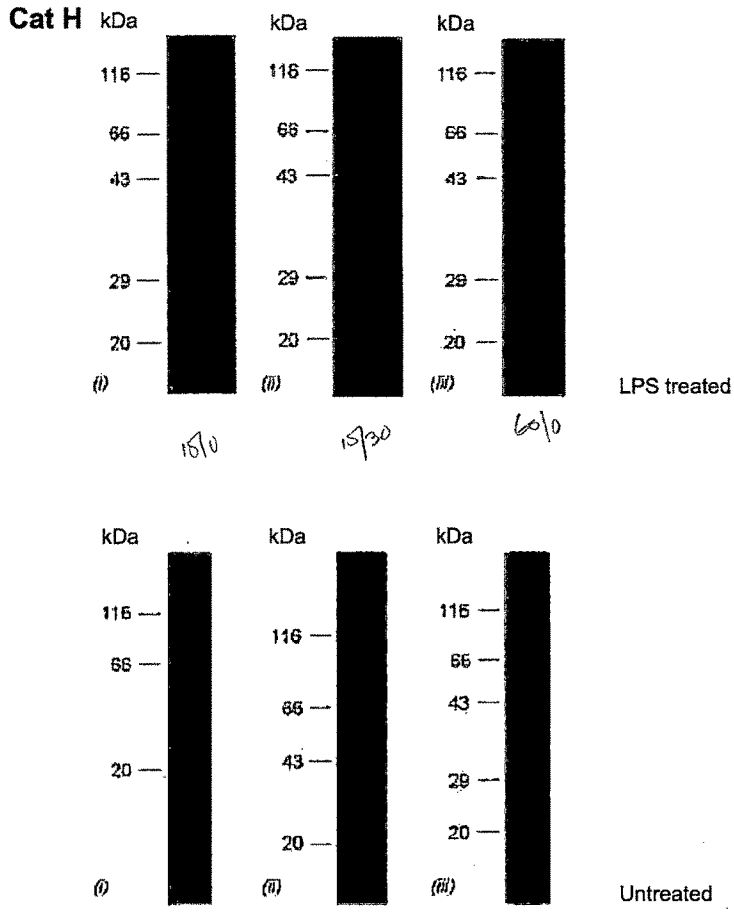

Fig. 14 a.

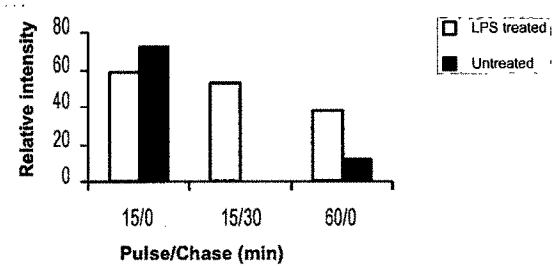

Fig. 14 b.

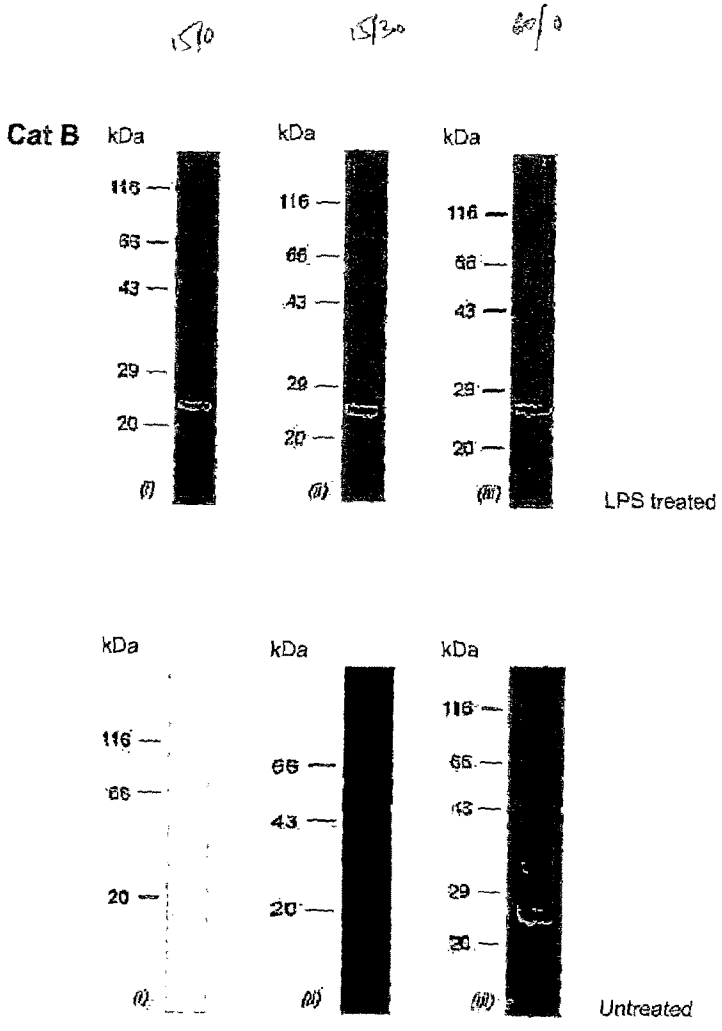

Fig. 15 a.

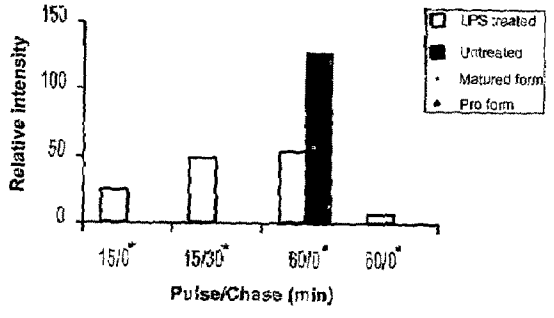

Fig. 15 b.

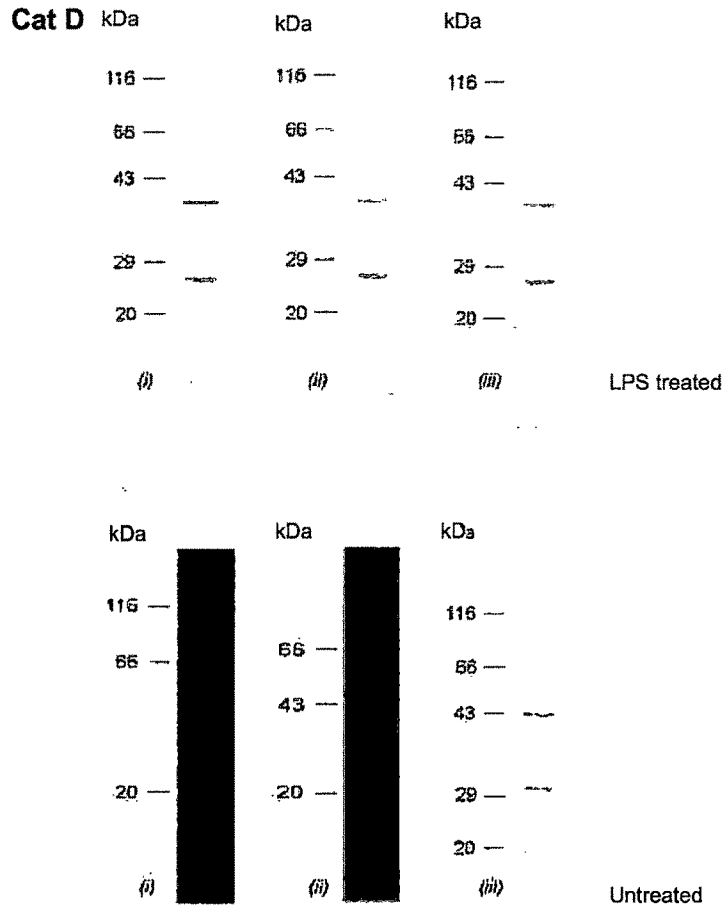

Fig. 16 a.

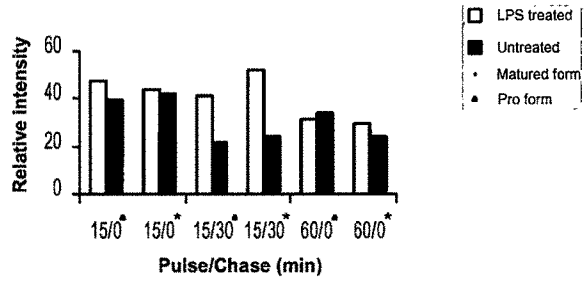

Fig. 16 b.

3.2.9 Immunofluorescence confocal microscopy

Analysis of U937 macrophage cells stimulated by LPS and unstimulated control under different conditions (described in section 2.3.8) showed excellent uptake of signals for FITC-dextran (Fig.18) The fluorescence observed in cells pulsed for 10 min without chase (set a - b and set c - d) appeared more concentrated at the edges of the cells compared to cells chased for longer periods (set e - f and set g - h), where the fluorescence intensity was more perinuclear.

Immunohistochemistry of pulsed and pulsed-and-chased cells demonstrated localization of Rab 5 and Rab 7. In control cells pulsed for 10 min without chase [Fig.18(a i, ii, iii)], Rab 5 was significantly higher compared to cells chased for 40 min [Fig.18(e i, ii, iii)]. Overlay analysis revealed significant co-localization of Rab 5 and FITC-dextran [Fig.18(a iii)]. Very few Rab 7 positive vesicles were detected in these cells pulsed for 10 min without chase [Fig.18(b i, ii, iii)]. However when cells were chased for 40 min after pulse, significant Rab 7 immunostaining was observed that co-localized with FITC-dextran [Fig.18(f i, ii, iii)].

In parallel cells stimulated with LPS, the levels of FITC-dextran uptake were comparable to control cells (set a, b and set c, d; set e, f and set g, h). Similar to that observed in control cells, Rab 5 immunoreactivity was prominently present in LPS stimulated cells pulsed for 10 min without chase; besides, the signal showed significant co-localization with FITC-dextran [Fig.18(c i, ii, iii)]. The signal for Rab 7 was insignificant in these cells as observed in control cells [Fig.18(d i, ii, iii)]. However in contrast to control cells, LPS stimulated cells chased for 40 min, showed significant signal for Rab 5 which co-localized with FITC dextran [Fig.18(g i, ii, iii)] and showed no detectable signal for Rab 7 [Fig.18(h i, ii, iii)].

3.2.10 Analysis of endosomal lipids

Lipids from PNS fractions and corresponding RF were effectively resolved by TLC system described in section 2.3.9a. The solvent systems employed, efficiently resolved the constituent polar and non polar lipids of the samples. Analysis of the TLC plates by the Camag TLC Evaluation Software™ allowed identification and quantitation of the resolved lipids against appropriate standards.

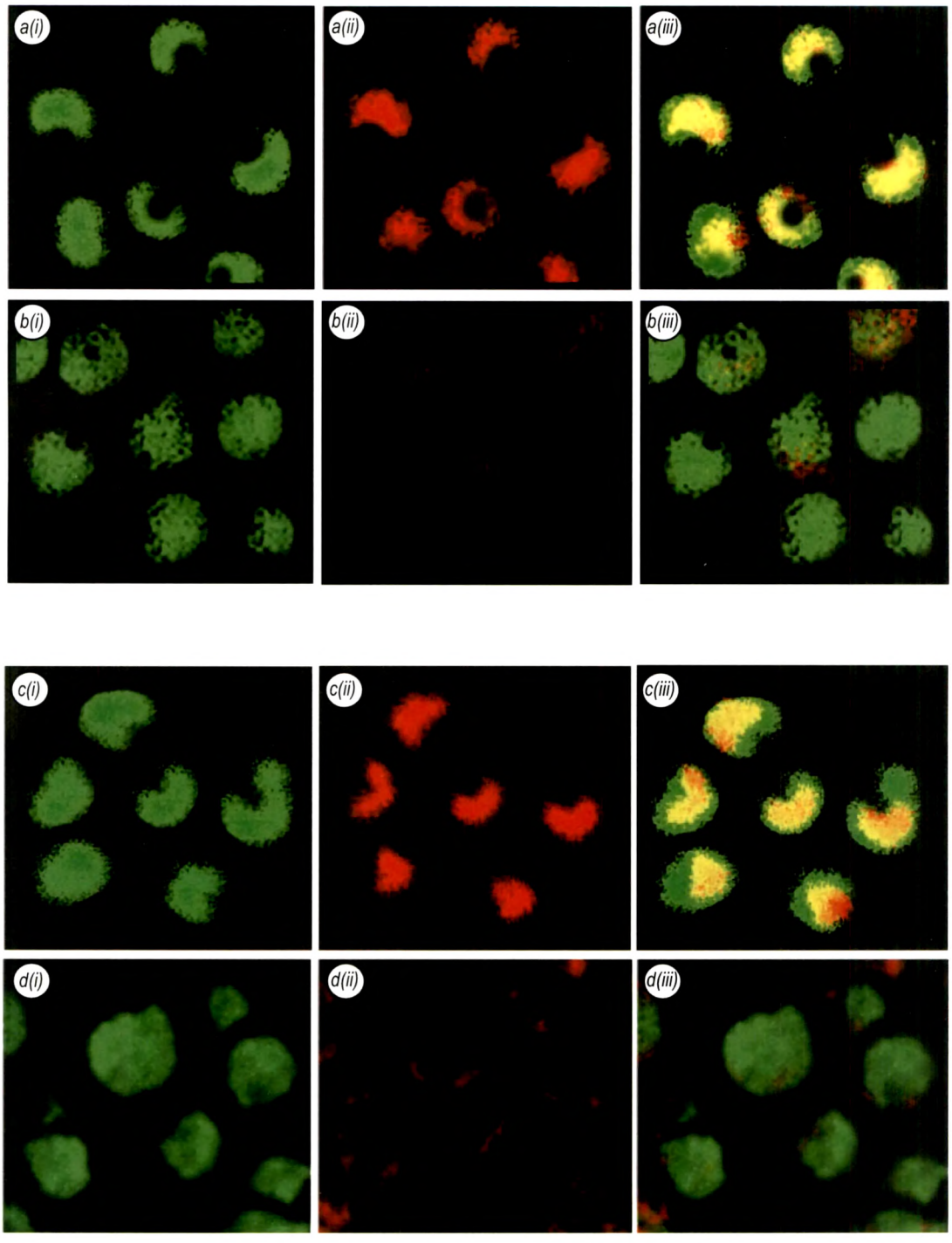

Fig. 18

continued in next page →

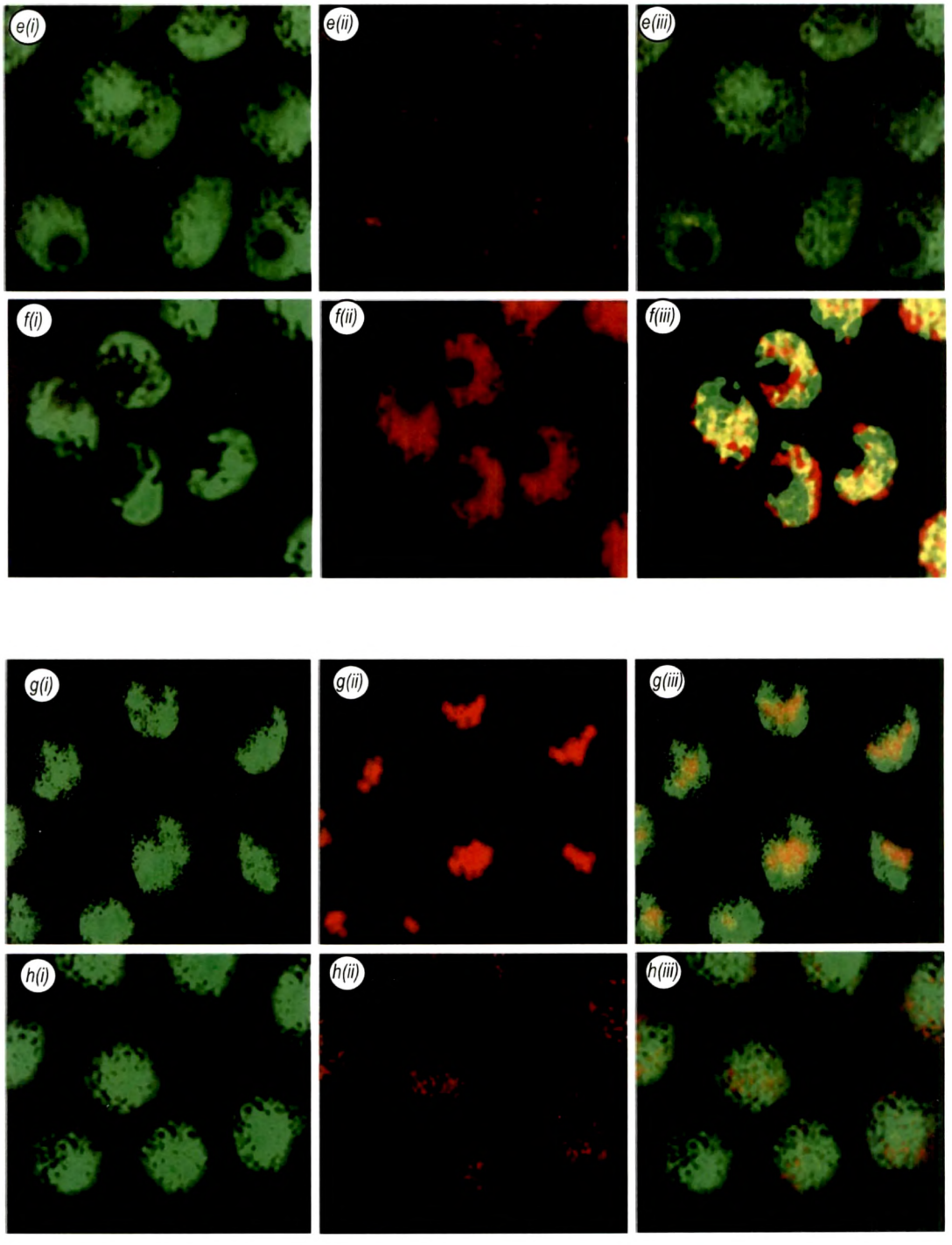

Fig. 18

→ continued from last page.

A. Lipid profile of 60'/0' pulsed samples

Analysis of the lipid profiles of the PNS and RF of the 60'/0' pulsed set, determined cholesterol as the most abundant lipid contributing ~52% and ~46% of the total lipids in PNS and RF respectively. Although, there was no major difference between the types of constituent lipids in either sample, the relative level of the lipids exhibited interesting variations (Table 9). Phosphatidylglycerol was present only in the endosomal samples while phosphatidic acid, phosphatidylinositol, phosphatidylserine, sphingomyelin and fatty acids like stearic acid were not detected in either PNS or RF. Phosphatidylcholine and phosphatidylethanolamine were the major phospholipids in endosome rich RF, representing 11.28% and 3.77% of the total phospholipids, respectively. Whereas fatty acids like oleic acid, was only 4.27% of the total lipid constituent of PNS, the latter fatty acid accounted for 13.11% of the lipid in RF (~3 - fold enrichment). Overall, phosphatidylethanolamine, phosphatidylcholine and phosphatidylglycerol were the major phospholipid constituents; while oleic acid was the major fatty acid constituent of RF. Interestingly, three lipids did not co-migrate with standards (uncharacterized lipid – 'UC'); two of these were selectively enriched in RF. The TLC and comparative histogram profiles for the corresponding lipids, between PNS and RF of 60'/0' pulsed cells are shown in Fig.19(a,b) respectively. Chromatogram and spectrum of the lipids are shown in Fig.19c(I,II).

B. Lipid profile of 15'/0' pulsed samples

Similar to the lipid profiles of the 60'/0' set, analysis of lipids from 15'/0' pulsed cells determined cholesterol as the most abundant lipid contributing 30% of the total lipids in PNS and RF (Table 10). Phosphatidylinositol was present only in PNS fraction and not detected in RF. Whereas 7.63% of the total PNS phospholipid was phosphatidylcholine, the latter constituted only 2.11% of RF lipids which indicated a 3.6 - fold difference. Similarly, 5.35% of PNS lipid was phosphatidylserine vs 2.11% of RF lipid, 2.6 - fold difference. In contrast to the higher levels of the above lipids in the PNS fraction, spingomyelin was enriched 2 - fold in RF. The phosphatidylcholine: phosphatidylethanolamine ratio was significantly higher in RF than in PNS. Overall,

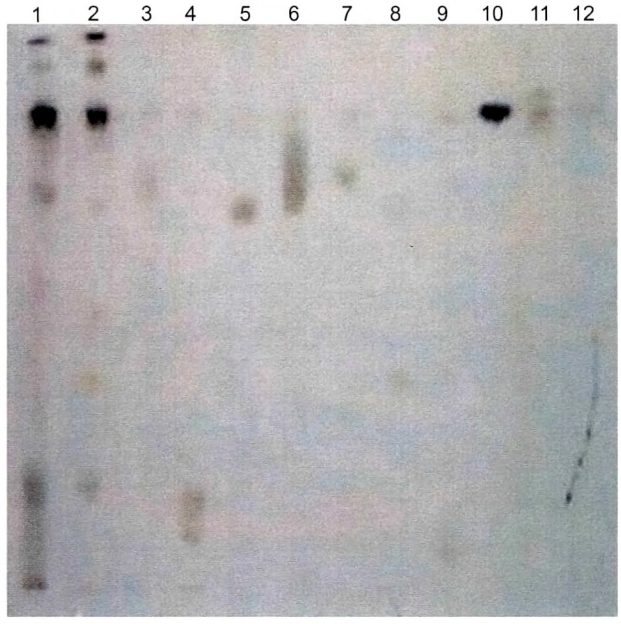

Fig. 19 a.

Lipid	% of Total lipids	
	PNS	RF
Phosphatidicacid	0	0
Phosphatidylcholine	18.41	11.28
Phosphatidylethanolamine	11.46	3.77
Phosphatidylglycerol	0	0.33
Phosphatidylinositol	0	0
Phosphatidylserine	0	8
Spingomyelin	0	0
Cholesterol	51.93	45.97
Oleicacid	4.27	13.11
Stearicacid	0	0
Uncharacterised *(UC)*	0. 5	6.66
Uncharacterised *(UC)*	4.92	0.46

n.d = Not detected

Table 9

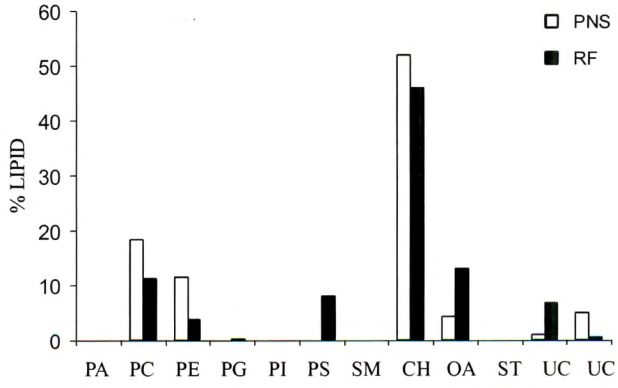

Fig. 19 b.

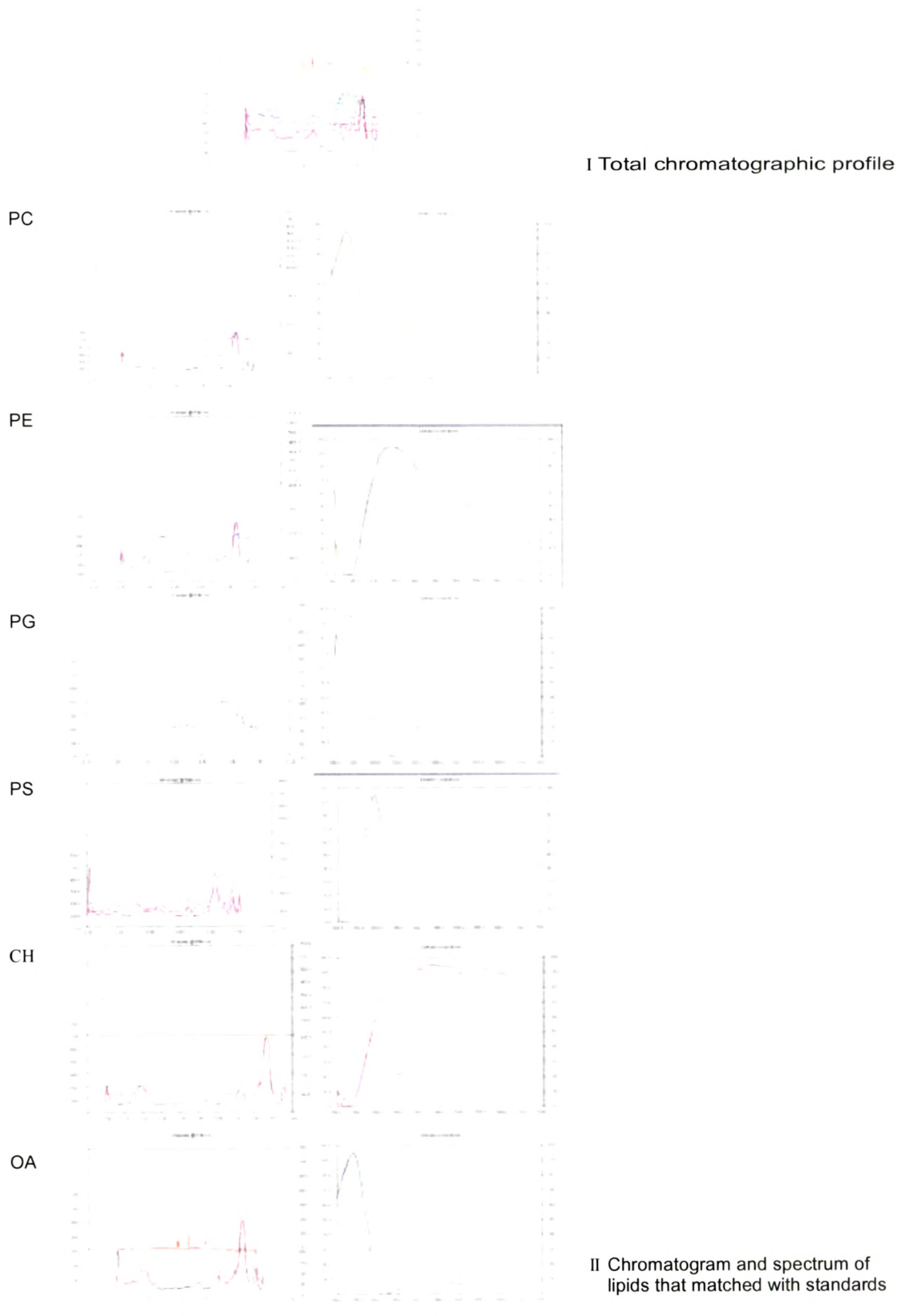
I Total chromatographic profile
PC
PE
PG
PS
CH
OA
II Chromatogram and spectrum of lipids that matched with standards
i
ii

Fig. 19 c.

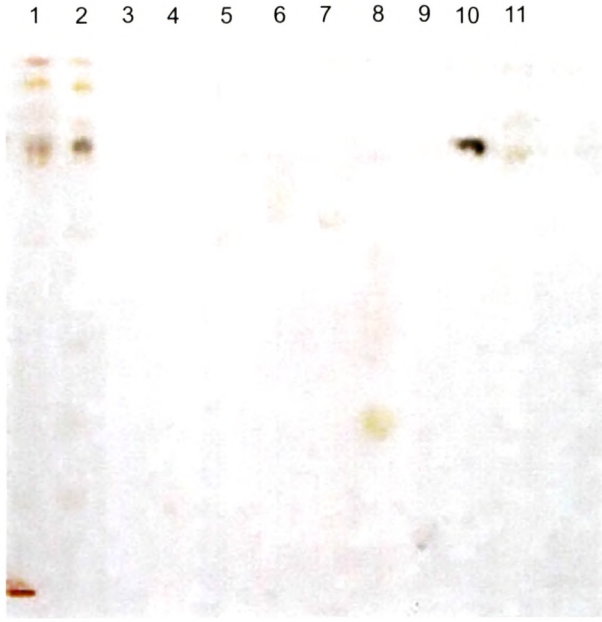

Fig. 20 a.

Lipid	% of Total lipids	
	PNS	RF
Phosphatidicacid	0	0
Phosphatidylcholine	7.63	2.11
Phosphatidylethanolamine	7.61	5.74
Phosphatidylglycerol	2.38	1.89
Phosphatidylinositol	2.86	0
Phosphatidylserine	5.35	2.11
Spingomyelin	1.24	2.54
Cholesterol	31.32	30.62
Oleicacid	10.05	8.85
Stearicacid	3.20	2.02
Uncharacterised	9.71	9.47

n.d = Not detected

Table 10

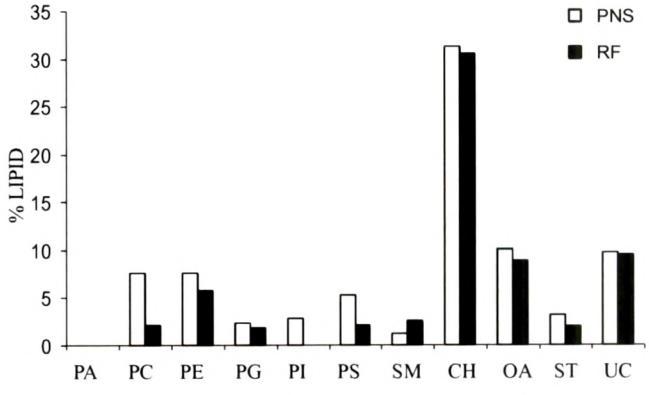

Fig. 20 b.

phosphatidylethanolamine, sphingomyelin, phosphatidylcholine and phosphatidylserine were the major phospholipid constituents of RF apart from the fatty acids. Interestingly, an uncharacterized lipid (UC) represented about 9.47% of the total endosomal lipids. The TLC and comparative histogram profiles for the corresponding lipids, between PNS and RF of 15'/0' pulsed sets are shown in Fig.20(a,b) respectively.

C. Lipid profile of 15'/60' pulsed samples

Analysis of the 15'/60' pulsed cells determined phosphatidylcholine, phosphatidylethanolamine and phosphatidylglycerol as the major phospholipids in endosomes, representing about 11.57%, 8.73% and 6.70% of the total lipids, respectively. Spingomyelin and phosphatidylserine, each about 5.83%, 5.22% respectively were also present. No phosphatidic acid, phosphatidylinositol and fatty acids like stearic acid were detected in either PNS or RF. Most abundant was cholesterol, which contributed up to 28% of the total endosomal lipid while fatty acids like oleic acid accounted for 2.61% of the total. Comparison of the lipid profile of PNS and RF showed the latter was enriched in phosphatidylglycerol (1.22 - fold), phosphatidylserine (5.22 - fold) and an uncharacterized lipid (4.26 - fold). Phosphatidylcholine, phosphatidylethanolamine, spingomyelin and chlolesterol levels were comparable in both PNS and RF (Table 11). The TLC and comparative histogram profiles of the corresponding lipids, from PNS and RF of 15'/60' pulsed cells are shown in Fig.21(a,b) respectively.

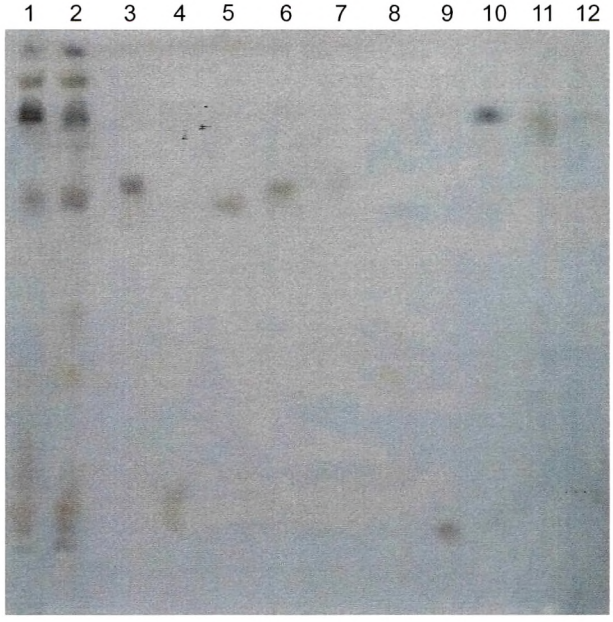

Fig. 21 a.

Lipid	% of Total lipids	
	PNS	RF
Phosphatidicacid	*n.d.*	*n.d.*
Phosphatidylcholine	12.50	11.57
Phosphatidylethanolamine	8.82	8.73
Phosphatidylglycerol	5.47	6.70
Phosphatidylinositol	*n.d.*	*n.d.*
Phosphatidylserine	*n.d.*	5.22
Spingomyelin	5.57	5.83
Cholesterol	33.4	28.13
Oleicacid	4.05	2.61
Stearicacid	*n.d.*	*n.d.*
Uncharacterised	*n.d.*	4.26
Uncharacterised	5.27	*n.d.*

n.d = Not detected

Table 11

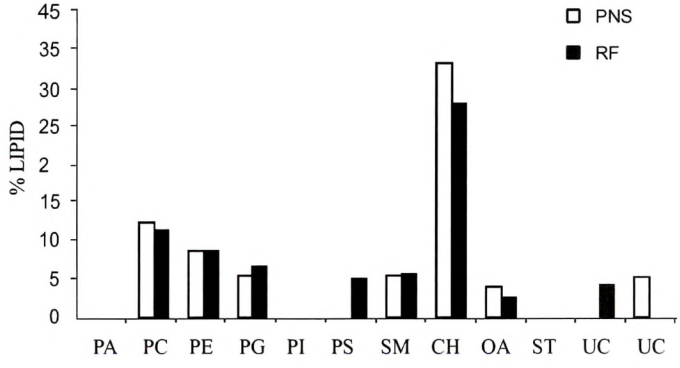

Fig. 21 b.